ABSTRACT

Title of Document: CYTOLOGICAL LOCALIZATION OF HEME IN *CAENORHABDITIS ELEGANS* USING MICROSCOPY

Cornelia Ellefson Kelley, Masters degree, 2007

Directed By: Dr. Iqbal Hamza, Assistant Professor, Department of Animal and Avian Sciences

This study was designed to develop an *in situ* histochemical heme staining method for an intact animal using the free-living nematode *Caenorhabditis elegans*. Although, heme is vital to many biological processes and synthesized by most known free-living organisms, *C. elegans* is a natural heme auxotroph. Using the substrate 3-3' diaminobenzidine and hydrogen peroxide, we used *C. elegans* to study the fate of heme. We found a direct correlation between heme in the growth medium and the organismal heme content. In addition, our studies confirmed that parents exposed to different heme levels contribute varying maternal heme to their progeny. Moreover, this methodology detected differences in heme levels between wild-type and mutants in heme homeostasis. Finally, we provide preliminary evidence that the technique can be applied to analyze heme-based structures at the electron microscopy level. Our studies described herein will aid in the characterization of heme transport pathways in eukaryotes.

CYTOLOGICAL LOCALIZATION OF HEME IN *CAENORABDITIS ELGANS* USING MICROSCOPY.

By

Cornelia Ellefson Kelley

Thesis submitted to the Faculty of the Graduate School of the
University of Maryland, College Park, in partial fulfillment
of the requirements for the degree of
Master of Science
2007

Advisory Committee:
Assistant Professor Iqbal Hamza, Chair
Professor Ian Mather
Professor Tom Porter

Dedication

To my loving husband and precious daughter

Acknowledgements

Thank you to my advisor Iqbal, from whom I've learned such an incredible amount during my time here.

To the other two members of my thesis committee, Ian and Tom. Thank you for your guidance.

To my wonderfully patient lab mates from whom I learned so much: Anita, Abbhi, Caiyong, Melissa, Caitlin, Suji, Scott, Jason, and Sandy. Thank you especially to Anita, Abbhi, Caitlin, and Scott who offered such valuable feedback on my literature review. Thank you all for putting up with me!

Thank you to my family: my parents and sisters for all their encouragement and support. Thank you especially to my mother whose numerous long trips from home to take care of her grandbaby were a tremendous help to Doug and myself.

To all the graduate students of this department upon whose friendship, sense of humor, and advice I relied on throughout my time here.

To all my family and friends who were so wonderfully supportive and never hesitated to lend a hand: Dad, Julia, Laura, Ann, Conoly, Melanie, Haynes, Jennifer, and Karin.

To Jessie, for being the most wonderful and precious daughter any mother could ask for.

And finally to my husband Doug, if not for his loving support, encouragement, and patience this would not have been possible.

Table of Contents

List of Tables

List of Figures

List of Abbreviations

ALA	δ–aminolevulinic acid
ALAS	δ–aminolevulinic acid synthase
IRR	Iron response regulator
Sre1p	Sterol regulatory element binding protein
NPAS2	Neuronal Pas domain protein 2
BMAL1	Brain and muscle arnt-like protein-1
IRE	Iron responsive element
IRP	Iron responsive protein
CDK	Cyclin-dependent kinase
NGF	Nerve growth factor
DGCR8	DiGeorge critical region-8
HO	Heme oxygenase
Hb	Hemoglobin
RBCs	Red blood cells
OGC	2-Oxoglutarate carrier
FLVCR	Feline leukemia virus subgroup C cellular receptor
PdTCPP	Palladium,meso-tetra[4-carboxyphenyl]porphyrin
PdTCPP	Palladium, meso-tetra(4-aminophenyl)porphyrin
PdMP	Palladium–mesoporphyrin IX
EM	Electron microscope
N2	*C. elegans* wild-type strain
IQ1068d	Mutant worm strain IQ1068 *dumpy*
DAB	3-3' diaminobenzidine
mCeHR	Modified *Caenorhabditis elegans* Habitatation and Reproduction
D	Day(s)
H	Hour(s)
Min	Minutes
PBS	Phosphate buffered saline
SOD	Superoxide dismutase
CAT	Catalase

Chapter 1: Literature Review

Introduction

The porphyrin, heme is one of the most biologically diversified molecules in nature. Heme functions as a prosthetic group in hundreds of proteins including the globins, respiratory cytochromes, cytochrome P450s, and thyroperoxidases, all proteins vital to processes such as oxygen transport, xenobiotic detoxification, oxidative metabolism, and thyroid hormone synthesis (1). In addition to functioning as a prosthetic group for a wide variety of proteins, heme also directly regulates biological processes such as cellular differentiation, cell cycle progression, and gene regulation (2,3). Most eukaryotes and prokaryotes synthesize heme in a highly conserved eight-step biosynthetic pathway. Regulation of heme biosynthesis has been extensively studied in many organisms including bacteria, yeast, and mammals (4-6). In humans, a deficiency in any of the enzymes of the heme biosynthetic pathway can lead to diseases known as the porphyrias.

There is a considerable amount of information known about eukaryotic heme biosynthesis and the wide-range of heme's functions in eukaryotes, however, very little is known about how this molecule is transported into cells, within cells, and into cellular organelles. While there have been studies that traced heme absorption in mammalian intestinal cells (7,8), only recently has research begun to identify proteins involved in eukaryotic heme uptake and transport (9-12). Once heme is synthesized in the mitochondria, some of it is used for incorporation into mitochondrial

hemoproteins. The rest of the newly synthesized heme must be transported out of the mitochondria for incorporation into hemoproteins located in the cytosol, nucleus, endoplasmic reticulum, and other organelles in order to participate in various cellular processes. Heme is hydrophobic and cytotoxic and can cause extensive cellular damage due to its inherent peroxidase activity. Thus, a *prima facie* argument can be made that heme likely does not exist free in cells. Understanding the fundamental biological process of eukaryotic heme trafficking has wide-ranging implications for solving pressing human, livestock, and crop health issues. From a human nutritional standpoint, dietary heme is the most bioavailable form of iron, but the heme absorption pathway(s) into intestinal cells is unknown. From a disease standpoint, helminthic infections are a tremendous burden to humans and livestock. Recent research indicates that several species of infectious nematodes are heme auxotrophs, i.e. they cannot synthesize heme but acquire it from diet (13). Discovery of heme transport pathway genes unique to these helminths could lead to the development of new pharmaceuticals to control helminthic infections.

Several techniques have been developed to cytologically localize heme and characterize its absorption into and transport within cells. Many methods involve the use of fluorescent dyes (14), fluorescent heme analogs (15), and radioisotopes (16), but one well-established method can be used to directly stain heme. This staining method involves the use of the compound 3-3' diaminobenzidine (DAB) and exploits the peroxidase activity of heme to generate a localized reaction product (17). Unpublished results have established that the non-parasitic nematode *C. elegans* is a natural heme auxotroph and thus provides an ideal model organism for studying heme

uptake (13). Establishment and examination of staining whole animals, such as *C. elegans,* for heme will provide a new approach to expand current knowledge of organismal heme homeostasis.

Heme biosynthesis

Heme biosynthesis occurs in a complex eight-step pathway conserved between eukaryotes and prokaryotes and can be broken down into several key processes (18). Briefly, a pyrrole ring is formed by two molecules of δ-aminolevulinic acid (ALA), followed by their assembly into a tetrapyrrole. Protoporphyrinogen IX is then formed by modification of the tetrapyrrole side chain and is subsequently oxidized to protoporphyrin IX. Iron is inserted into protoporphyrin IX in the final step to form protoheme, or heme *b,* the most common form of heme (18). Depending upon the hemoprotein for which heme is needed, heme *b* can then be modified to heme *a* or heme *c*.

The first step in eukaryotic heme biosynthesis occurs in the mitochondria and results in the formation of ALA, the universal porphyrin precursor, by a condensation reaction between succinyl CoA and glycine catalyzed by ALA synthase (ALAS), as seen in Figure 1. ALA is then transported out of the mitochondria into the cytoplasm. In the second step, two molecules of ALA form porphobilinogen in a condensation reaction catalyzed by aminolevulinic acid dehydratase, also known as porphobilinogen synthase. Four molecules of porphobilinogen are then used to form the unstable polymer hydroxymethylbilane in the third reaction catalyzed by porphobilinogen deaminase. Uroporphyrinogen III synthase then converts

Figure 1: Eukaryotic heme biosynthetic pathway.

The eight-step eukaryotic heme biosynthetic pathway begins with the synthesis of ALA in the mitochondria. ALA is then transported from the mitochondria into the cytosol, where the subsequent four steps occur. The heme precursor coproporphyrinogen III is transported back into the mitochondria for the final three steps culminating in the formation of protoheme (heme *b*).

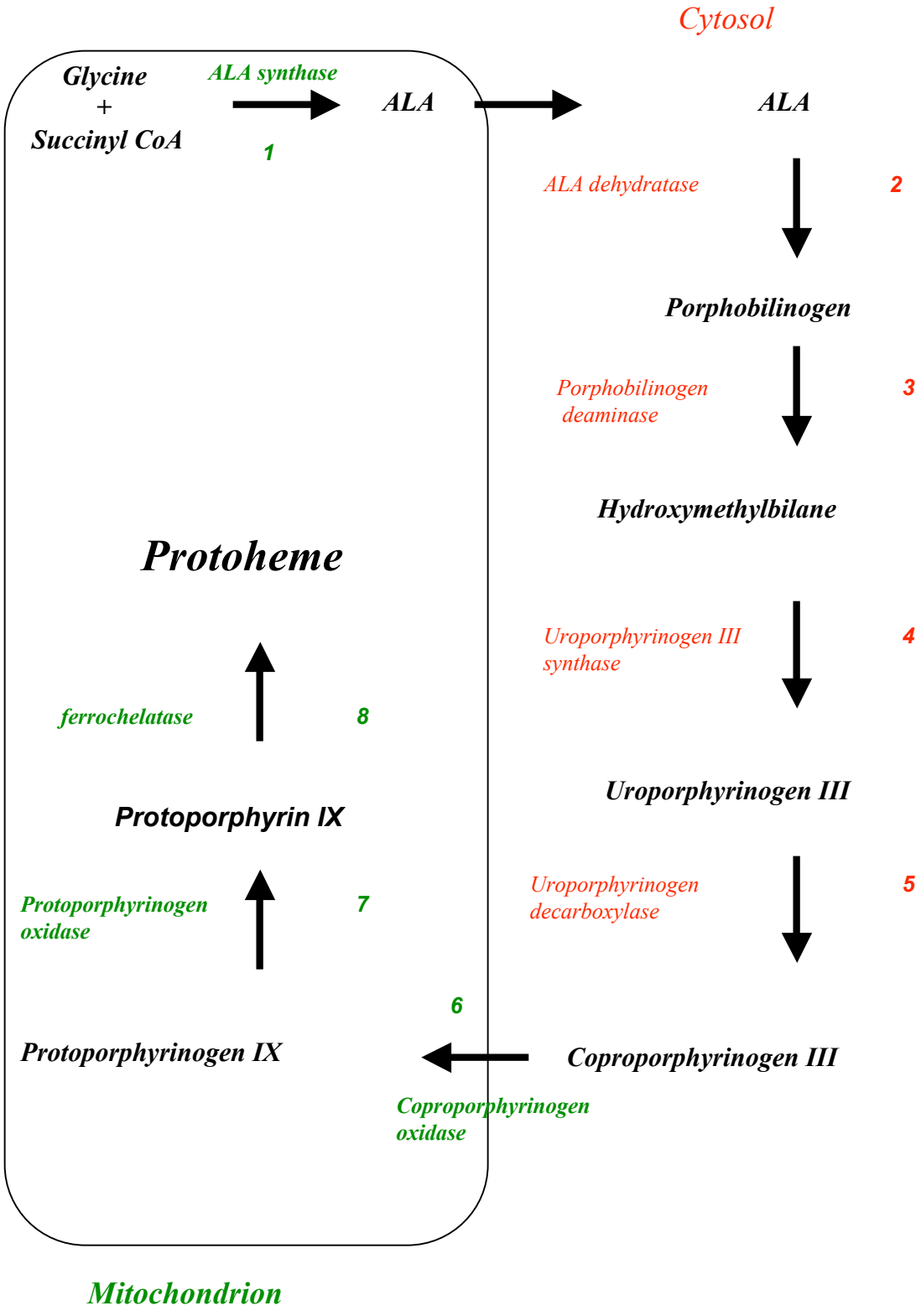
Cytosol
Glycine
+
Succinyl CoA
ALA synthase
1
ALA
ALA
ALA dehydratase
2
Porphobilinogen
Porphobilinogen deaminase
3
Hydroxymethylbilane
Uroporphyrinogen III synthase
4
Uroporphyrinogen III
Uroporphyrinogen decarboxylase
5
Coproporphyrinogen III
6
Coproporphyrinogen oxidase
Protoporphyrinogen IX
Protoporphyrinogen oxidase
7
Protoporphyrin IX
ferrochelatase
8
Protoheme
Mitochondrion

hydroxymethylbilane to uroporphyrinogen III during step four. Step five involves the conversion of uroporphyrinogen III to coproporphyrinogen III catalyzed by uroporphyrinogen decarboxylase. Coproporphyrinogen III is then transported back into the mitochondria where coproporphyrinogen oxidase, an enzyme located in the mitochondrial inner membrane, catalyzes the formation of protoporphyrinogen IX during step six. Next, protoporphyrin IX is formed by protoporphyrinogen oxidase. The final step occurs when ferrous iron is inserted into the protoporphyrin IX cyclic macromolecule to form heme *b*. This final reaction is catalyzed by ferrochelatase. Further modifications of heme *b* at C-2 and C-8 are required to form heme *a,* the form of heme found in cytochrome oxidases (19). Synthesis of heme *a* from heme *b* involves two enzymatic reactions. Heme O synthase catalyzes the conversion of the vinyl group to a 17-hydroxyethylfarnesyl to generate heme *o.* Heme *o* is then converted to heme *a* by heme A synthase (HAS) (20). Heme *c* is found in cytochromes *c1* and *c* and differs from heme *b* in that heme *c* covalently binds to its proteins through the two vinyl side chains (21).

While this biosynthetic pathway is highly conserved between eukaryotes and prokaryotes, there are a few differences. One obvious difference is that, in eukaryotes, the biosynthetic pathway is partially compartmentalized between the mitochondria and the cytosol, as demonstrated in Figure 1. Another difference is that some prokaryotes can synthesize ALA by an alternative pathway. These organisms synthesize ALA via the C-5 pathway, a pathway that converts glutamic acid to ALA acid glutamyl-tRNA and glutamate semialdehyde as intermediates (22). No known prokaryote has the capability to synthesize ALA using both the C-5 pathway and the

ALAS pathway. One other notable difference between eukaryotes and prokaryotes is that eukaryotic heme demand requires heme to be both exogenously acquired as well as endogenously synthesized, while prokaryotic heme demand is usually met by heme biosynthesis (23).

Regulation of heme biosynthesis

Regulation of heme biosynthesis has been studied in many different model systems and varies from organism to organism. In some organisms, heme biosynthesis is connected to iron availability (4,18), while, in others, regulation can depend on oxygen levels (5). In the yeast *Schizosaccharomyces pombe*, Sterol Regulatory element binding protein (Sre1p) up-regulates six heme biosynthetic pathway enzymes during anaerobic conditions (5). It is thought that Sre1p maintains heme levels under oxygen-limiting conditions.

In the bacterium *Bradyrhizobium japonicum,* heme biosynthesis is coordinated to iron availability (4). Iron is inserted in the protoporphyrin IX ring by ferrochelatase during the final step of the heme biosynthetic pathway. During iron deficiency, bacterial cells with a mutation in the iron response regulator (IRR) gene are unable to arrest the heme biosynthetic pathway and accumulate toxic levels of protoporphyrin IX. This protein coordinates heme biosynthesis to iron availability. Additional studies showed that IRR inhibits the heme biosynthetic pathway by inhibiting *hemB*, the gene encoding ALA dehydratase in *B. japonicum*. Under iron limiting conditions, IRR inhibition of *hemB* ultimately prevents toxic accumulation of protoporphyrin IX in wild-type organisms (4).

In mammals, it is the first step of heme biosynthesis, catalyzed by the enzyme ALAS, that is highly regulated. Mammals differ from other organisms in that they require two different forms of ALAS. While heme biosynthesis occurs in every cell, the majority of heme biosynthesis occurs in the bone marrow for incorporation into hemoglobin. This increased demand for heme biosynthesis in the bone marrow requires a separate form of ALAS, ALAS2. *ALAS2* is expressed only in erythroid cells, in the bone marrow (24), while *ALAS1* encodes the constitutively expressed form of ALAS. Regulation of heme biosynthesis in erythroid cells via *ALAS2* is thus separate from regulation of constitutive biosynthesis at the level of *ALAS1* (18).

In mammals, the main transcriptional regulator of *ALAS1* is neuronal Pas domain protein 2 (NPAS2), a mammalian transcription factor known to be part of the core circadian clock mechanism (6). NPAS2 is a PAS domain protein, a family of proteins that can detect environmental signals such as oxygen and light, as well as small aromatic molecules, including heme (25). NPAS2 has two PAS domains, each of which bind heme, and the ability of NPAS2 to bind DNA is dependent on heme availability. When NPAS2 binds heme, it forms a heterodimer with BMAL1, and this transcription complex binds the *ALAS1* promoter. Expression of *ALAS1* is then upregulated, thus inducing heme biosynthesis (6). Excess heme in the cell induces heme oxygenase, the enzyme responsible for degrading heme into carbon monoxide, biliverdin, and iron. In the presence of carbon monoxide, the NPAS2 –BMAL1 transcription complex cannot sufficiently bind DNA, thus preventing expression of *ALAS1* (25).

In erythroid cells, *ALAS2* is transcriptionally regulated by histone

acetyltransferase p300 (26). This transcriptional regulator is recruited by the erythroid specific transcription factor, GATA1. The interaction of these two proteins activates the *ALAS2* promoter (27). Translational regulation of ALAS2 in murine erythroleukemia cells is regulated in an iron–dependent manner by the Iron Responsive Element/ Iron Responsive Protein (IRE/IRP) system (28). When iron is low, IRP binds to the IRE of the 5' untranslated region of the ALAS2 mRNA transcript, inhibits translation and prevents heme synthesis in these erythroid cells. While IRP exists in two forms, IRP1 and IRP2, only IRP2 translationally regulates ALAS2 (29). IRP2 knockout mice overexpress *ALAS2* and have elevated levels of free protoporphyrin IX in their red blood cells, which is possibly responsible for observed phenotypes that include photosensitivity, skin and eye lesions (29).

Deficiencies in heme biosynthesis

Any deficiency in ALAS2 or the other seven enzymes in this pathway can cause the porphyrias. Porphyrias are a family of diseases that cause neuropsychiatric symptoms including anxiety, insomnia, confusion, hallucinations, agitation and paranoia (30). Porphyria attacks could occur because a) heme deficiency leads to deficiency of hemoproteins critical to cellular function, or b) enzyme defects cause toxic levels of pathway intermediates to accumulate, resulting in a neurotoxic effect (30). An additional explanation is that heme deficiency results in decreased production of microRNAs, a class of RNAs vital to many diverse biological processes. Recently, microRNA processing was shown to involve heme (3). Heme deficiency could have a global effect by impacting a number of biological processes.

Hemoproteins

Once heme is endogenously synthesized or exogenously acquired, it must then be transported to the cytoplasm or cellular organelles for insertion into any of the hemoproteins vital to cellular function. The cytochrome P450 enzymes are hemoproteins whose primary role is xenobiotic detoxification. Xenobiotics are foreign chemicals found in an organism that must be safely metabolized and excreted. Food additives, industrial chemicals, pesticides, plant toxins and pharmaceutical agents are common xenobiotics. Deamination, desulfuration, hydroxylation, and oxidation reactions catalyzed by cytochrome P450s allow cells to metabolize xenobiotics into a form that can be excreted (31). In yeast and humans, cytochrome P450s are required for sterol biosynthesis. It was discovered recently that the eukaryotic hemoprotein Dap1 binds several endoplasmic reticulum cytochrome P450 proteins in both humans and yeast and that Dap1 is essential for sterol biosynthesis (32).

Another family of hemoproteins is the heme-based sensor family. These proteins are key regulators of adaptive responses to changing levels of oxygen, carbon monoxide, and nitric oxide. Proteins are classified as heme-based sensors because one protein domain is controlled by a heme-binding domain within the same protein (25). There have been more than fifty heme-based sensors studied in bacteria and mammalian cells (26). One example of a mammalian heme-based sensor is soluble guanylyl cyclase. This cytosolic protein synthesizes cyclic guanosine monophosphate (cGMP) from guanosine triphosphate (GTP) when it can detect

nitrous oxide and carbon monoxide. cGMP then acts on downstream effectors that control smooth muscle tone and neurotransmission among other physiological processes (26).

Heme is vital to cellular respiration because several key hemoproteins are involved in energy production (1). These hemoproteins are the respiratory cytochromes, electron-transferring proteins located in the mitochondrial inner membrane. The iron atom at the center of the heme ring alternates between a reduced ferrous state and an oxidized ferric state during electron transport reactions. Two of these mitochondrial protein complexes are cytochrome reductase complex (complex III) and cytochrome *c* oxidase (complex IV). The cytochrome reductase complex contains three heme prosthetic groups, while complex IV, or cytochrome *c* oxidase, has two heme prosthetic groups (1).

Hemoproteins are also involved in thyroid hormone synthesis (33). Thyroperoxidase is a membrane-bound hemoprotein that catalyzes the production of the thyroid hormones, thyroxine (T_4) and 3,3' 5-triiodothyronine (T_3). The trafficking of thyroperoxidase to the cell surface from the endoplasmic reticulum and subsequent enzymatic activity is dependent on insertion of heme into apo-thyroperoxidase. Heme must therefore be transported into the ER for incorporation into thyroperoxidase. Inhibition of heme biosynthesis significantly reduces thyroperoxidase trafficking to the cell surface and its subsequent enzymatic activity (33).

Heme as a regulator

Heme also plays a regulatory role in many biological processes including cell growth, cell cycle progression, cellular differentiation, gene regulation, and microRNA processing. This regulatory role can be cell-type specific. While heme promotes cell growth and cell cycle progression in HeLa cancer cells, it promotes cellular differentiation in PC12 pro-neuronal cells and K562 erythroid cells (2).

In HeLa cells, heme directly controls the cell cycle by acting on two key cell cycle regulators, cyclin-dependent kinases (CDKs) and p53 (34). CDK proteins promote cell cycle progression, while p53 suppresses cell growth by activating cell cycle suppressor proteins and inducing BAX and Fas, two proapoptotic genes. When DNA in a cell becomes damaged, the functional protein product of *p53* induces the transcription of *p31*, whose protein product blocks the activity of CDK complexes. Inhibition of CDK complexes prevents the cell from progressing to the S-phase of the cell cycle, preventing damaged DNA from replicating. When heme biosynthesis was inhibited in HeLa cells, they arrested in the S phase of the cell cycle and this cell cycle arrest was accompanied by morphological changes associated with senescence. Addition of heme reversed these effects. Inhibiting heme synthesis increased p53 levels four to five fold, an effect that was reversed when heme was added back to the medium, suggesting that heme has a direct effect on p53. Conversely, inhibiting heme biosynthesis decreased the cellular levels of three CDK proteins: Cdk4, Cdc2, and cyclin D4. Adding heme to these cells again reversed these effects (34).

In PC12 cells and red blood cells, heme plays a role in cellular differentiation.

Heme is critical for neuronal differentiation via the Ras-ERK 1 and 2 signaling pathways (2). Heme deficiency inactivates the Ras-ERK signaling pathways that are induced by nerve growth factor (NGF), a protein secreted by neurons that plays a crucial role in the differentiation of neural crest-derived sensory and sympathetic neurons. Heme deficiency caused NGF-differentiated PC12 cells to undergo caspase activation and subsequent apoptosis. Experiments also showed that undifferentiated PC12 cells were less vulnerable to heme deficiency. This disparity in heme deficiency vulnerability between differentiated and undifferentiated cells suggested a role for heme in NGF signaling (2). Additionally, male mouse embryos hemizygous for *ALAS2* die at embryonic day 11.5 due to severe anemia. The primitive erythroid cells did not mature, suggesting an additional role for heme in erythroid cellular differentiation (24).

In addition to a direct role in controlling the cell cycle and cellular differentiation, heme also has an indirect role in regulating developmental timing processes, cellular differentiation, and apoptosis through its involvement in microRNA production (3). MicroRNAs are short RNAs, generally twenty-two nucleotides long, that play a significant role in regulating protein-encoding genes. Ten to thirty percent of all protein-encoding genes are regulated by microRNAs. Recently, it was shown that heme plays a role in the activation of a protein critical to microRNA processing. This protein, DiGeorge critical region-8 (DGCR8), requires heme for dimerization and subsequent activation. After DGCR8 dimerizes, it binds to primary microRNAs, and the resulting trimer triggers cleavage of the primary microRNA by DROSHA to produce mature microRNAs (3). This particular

regulatory role for heme could have severe ramifications for cells during heme deficiency. In this case, heme deficiency would result in a reduction of mature microRNAs, an effect that could seriously impact multiple cellular processes.

Recent work suggests that there is reciprocal regulation between heme biosynthesis and the circadian clock (6). Circadian clocks play a crucial role in regulating physiology and behavior in organisms ranging from plants to animals (35). Research indicates that heme control of the circadian clock complex is transcriptionally regulated (6). In *Drosophila,* the *dperiod* gene is an intrinsic part of the animal's circadian clockwork. Two *dperiod* homologs, *mPER1* and *mPER2* regulate the mammalian circadian clock. In mice, heme was shown to decrease expression of *mPer2* but increase expression of *mPer1,* an effect most pronounced when the mice were subjected to complete darkness. These results suggested involvement in the circadian clock. Further studies showed that the expression patterns of *mPer1* and *mPer2* were differentially heme-regulated by NPAS2 and mPER2, two circadian clock proteins that bind heme. When heme binds NPAS2, NPAS2 forms a transcription complex with BMAL1, a complex positively regulated by mPER2 *in vivo*. This complex activates the *ALAS1* promoter, thus inducing heme biosynthesis (6).

In yeast, heme regulates gene expression through the heme-responsive transcriptional regulator, Hap1p (5). In *S. cerevisiae,* Hap1p regulates the expression of ROX1, a gene that regulates expression of roughly one-third of all anaerobically expressed genes. Under aerobic conditions, ROX1 transcription is upregulated by Hap1p, and genes necessary for anaerobic conditions are repressed. Extracellular

oxygen levels determine heme synthesis in yeast, and, under long-term hypoxic conditions, oxygen-dependent heme synthesis decreases. This is followed by a decrease in HAP1p activity and subsequent down-regulation of ROX1, which allows the expression of genes needed for hypoxic conditions (5).

Hap1p is also involved in steroid biosynthesis in yeast in two ways. One is by regulating HMG1, one of the genes in the sterol biosynthetic pathway, and the other is by playing a role regulating gene targets of the two transcription factors Upc2p and Ecm22p (36). Upc2p and Ecm22p activate the *ERG* genes, which are responsible for sterol biosynthesis in yeast. Under hypoxic conditions, Hap1p plays a role in regulating gene targets of Upc2p and Ecm22p, but precisely how it does this is not entirely clear. Basal expression of another sterol biosynthetic gene, *ERG2*, requires Hap1p, regardless of whether the expression was activated by Ecm22p or Upc2p. It is not clear whether sterols or heme are responsible for induction of these transcription factors under hypoxic conditions. However, hypoxic induction of *ERG* genes responds to heme levels rather than sterol levels, a response that does not involve either Upc2p or Ecm22p (36).

Heme degradation

While heme biosynthesis is absolutely essential to cellular function, heme degradation is also an important aspect of cellular metabolism. The main purpose of heme degradation is the reutilization of iron from hemoglobin (31). Heme is degraded by heme oxygenase (HO) to ferrous iron, carbon monoxide and biliverdin. There are two isoforms of heme oxygenase, *HO-1* and *HO-2*, each encoded by a

separate gene. *HO-2* is the constitutive form of heme oxygenase, while *HO-1* is highly inducible (2).

HO-1 is regulated by Bach1, a heme-regulated mammalian transcriptional repressor (37). In human hepatocytes, silencing Bach1 upregulates *HO-1* gene expression. Bach1 downregulates *HO-1* by forming heterodimers with Maf proteins and binding to the heme responsive elements (HeRes) in the 5' untranslated region of the *HO-1* promoter. Heme binds to Bach1, causing a conformational change that markedly decreases the ability of Bach1 to bind HeRe elements. When the Bach1 complex no longer binds these binding sites on the promoter, the sites can then be bound by the *HO-1* transcriptional activators, Maf-Maf and Nrf2-Maf (37).

Heme transport

Heme transport has been studied in a wide variety of organisms including bacteria, yeast, invertebrates, and mammals. However, this field of research has been complicated because many model organisms are heme prototrophs, i.e. they synthesize heme. Distinguishing between heme synthesized intracellularly and heme obtained from exogenous sources, therefore, is difficult without labeling one source of heme with fluorescent dyes, fluorescent molecules, or radioisotopes. While prokaryotic heme biosynthesis is sufficient for prokaryotic heme demand (23), many bacteria obtain heme from exogenous sources to utilize as a source of iron (38). Many proteins directly responsible for heme uptake and transport in bacteria have been identified and characterized (38).

In contrast to the field of bacterial heme transport, eukaryotic heme transport

proteins have been identified only recently. Two genes with homologs in other pathogenic yeast species are required for heme uptake in the yeast *Candida albicans* (39). In 2005, it was discovered that the model organism, *C. elegans* requires heme but does not synthesize it. While *C. elegans* is non-pathogenic, there are pathogenic nematodes that also require heme but are unable to synthesize it (13). These findings suggest that heme uptake could be an Achilles heel for some nematodes harmful to human, crop, and livestock health (13). The pathways for how heme is transported into cells from external sources, transported between cells, and transported within cells, remains to be identified.

Heme uptake has been well characterized in many bacterial species and the general mechanisms by which this occurs in gram-negative bacteria is demonstrated in Figure 2 (38). Gram-positive bacteria contain specific binding proteins anchored to the inner membrane that recognize heme sources. Once these heme sources are identified and bound, they are transported by ABC permeases.

The first involves direct contact between heme or heme binding proteins and an outer-membrane receptor while the second system involves the release of proteins known as hemophores into the extracellular media by the bacteria. The hemophores bind heme or heme-binding proteins such as hemoglobin and hemopexin, and deliver them to specific receptors located on the bacteria's outer membrane. The hemophore system has thus far been found only in gram-negative bacteria (40).

Two of these hemophore systems are the HxuA and HasA systems (38). The HxuA system is found in *Haemophilus influenza* and is the only bacterial system known to utilize heme bound to hemopexin (38). *H. influenza* does not synthesize

Figure 2: Heme acquisition by gram-negative bacteria.

Bacteria secrete hemolysin to degrade red blood cells (RBC's), releasing hemoglobin and heme with heme being bound by albumin or hemopexin. There are then three different ways in which the bacteria obtain the heme.

1 Heme and hemoglobin can bind directly to a TonB-dependent outer membrane receptor.

2 Bacteria release proteins called hemophores that capture hemoglobin and hemopexin. The hemophores then bind to specific TonB dependent outer membrane receptors.

3 Bacterial proteases, either membrane-bound or secreted, degrade hemoglobin, hemopexin, and albumin. This process releases heme that subsequently binds to specific TonB –dependent receptors and is released into the periplasmic space. Heme is then transported through the cytoplasmic membrane by a process that is not well described.

Once heme reaches the cytoplasm it is degraded by heme oxygenase, releasing iron and protoporphyrin IX (adapted from reference (38)).

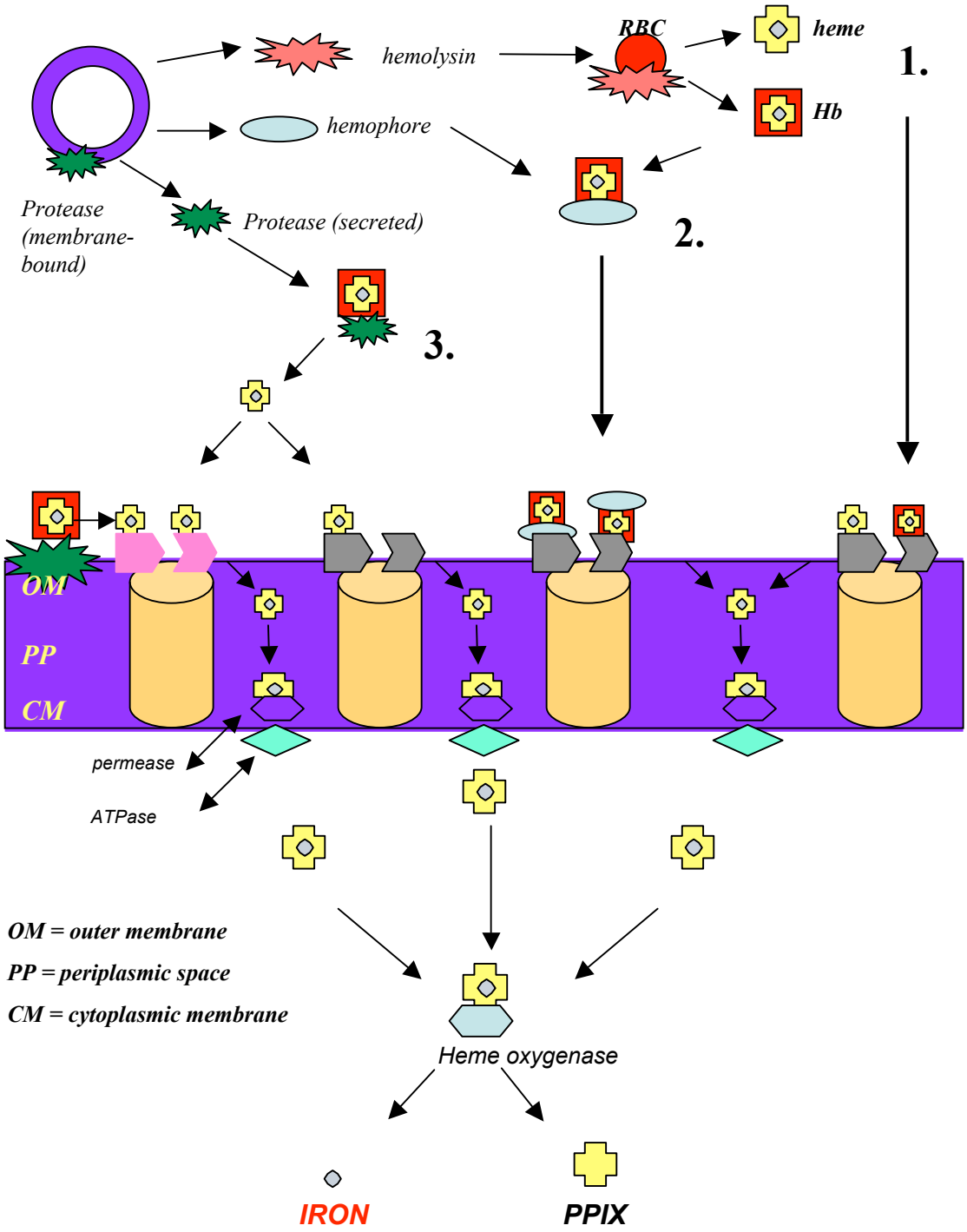
hemolysin
RBC
heme
Hb
1.
hemophore
2.
Protease (membrane-bound)
Protease (secreted)
3.
OM
PP
CM
permease
ATPase
OM = outer membrane
PP = periplasmic space
CM = cytoplasmic membrane
Heme oxygenase
IRON
PPIX

heme, and contains the *HxuABC* gene cluster that allows it to efficiently utilize hemopexin, a heme-binding blood plasma protein. HxuA is secreted, binds hemopexin and this complex binds to HxuA-hemopexin specific receptors. The HasA system is found in at least five bacterial species and functions by capturing free heme or heme from hemoglobin and presenting it to specific outer-membrane receptors (40).

Animals combat parasitic infections by limiting the amount of free iron in their blood. Because of this limited availability of iron, many pathogenic microorganisms have evolved heme acquisition pathways that allow them to use heme from their host as a source of iron, and at least one species of pathogenic bacteria prefers heme iron over iron bound to transferrin (41). Also, it has been shown that targeting heme uptake pathways of pathogenic bacteria can affect their virulency (41,42). Mutating genes involved in the heme uptake system of the bacteria responsible for whooping cough in humans, *Bordatella pertussis,* reduced its infective strength in the mouse because the organism's iron uptake systems were unable to compensate for the inability to acquire heme (42). Mutating the heme uptake pathway in the gram-positive bacterium, *Staphylococcus aureus,* reduced its infective strength in the worm model, *C. elegans* (41). While proteins involved in bacterial heme uptake and utilization have been studied extensively, only recently have proteins with similar functions been discovered in eukaryotes. Two recently discovered genes, *RBT5* and *RBT51,* are responsible for heme uptake in *C. albicans* (9). While these two proteins have a seventy percent identity to one another, *RBT5* plays the dominant heme acquisition role in *C. albicans*. However, *RBT5* does not

confer to another yeast species, *S. cerevisiae,* the ability to utilize hemoglobin as an exogenous iron source (9).

It was shown that Rbt5p and Rbt51p are heme receptors induced by iron starvation. While these genes allow *C. albicans* to utilize heme as an iron source, the underlying molecular mechanism is not known. One proposed mechanism is that these proteins facilitate the diffusion of heme through the plasma membrane. Another hypothesis is that Rbt5p could allow the heme to be taken up by a not-yet-discovered heme transporter. Alternatively, Rbt5/Rbt51 could be internalized from the plasma membrane with the heme where the heme is then released into the cytoplasm (9,43). In addition to *RBT5* and *RBT51, C. albicans* contains another gene essential to its ability to utilize hemoglobin as an iron source. The gene, CaHMX1, is a heme oxygenase that is twenty-five percent homologous to human heme oxygenase. While CaHMX1 is the first gene known in *C. albicans* to be regulated by heme (44) and mammalian hemoglobin (45), its exact enzymatic activities are not yet clear. While *C. albicans* can become pathogenic and use heme as an iron source, mutating genes responsible for heme uptake did not reduce its virulency in the mouse model. Two additional pathogenic yeast species, however, efficiently utilized heme as an iron source and the proteins responsible for this are homologous to Rbt51p, indicating a possible vulnerability of these pathogens to heme deficiency (9).

Worldwide, pathogenic nematodes cause significant problems for humans, crops, and livestock. One-third of Earth's human population is infected with soil-transmitted helminths and the majority of those infected live in the developing world (46) Large-scale drug treatment programs have been designed and implemented to

combat these helminthic infections in humans, increasing the likelihood of drug resistance. Although anthelmintic drug resistance in humans has not yet become a problem, wide-spread use of anti-helminths in the animal husbandry industry has led to rampant drug resistance (47). Recent studies suggest that a potential Achilles heel and novel pharmaceutical target for some of these parasites is heme uptake (13). When it was discovered that the non-parasitic model organism *C. elegans* is a natural heme auxotroph, further studies revealed that five other phylogenetically diverse species of parasitic nematodes also depend on heme acquisition from exogenous sources (13).

Another recently published report suggests that host dietary iron supply affects the ability of the hookworm *Ancylostoma ceylanicum* to infect its host (48). Hamsters infected with *A. ceylanicum* and fed a diet with severe iron restriction, had a significant reduction in the parasite load compared to animals that were fed a diet with moderate levels of iron. These results suggest that hookworms rely on the host iron to maintain growth and development. Host iron deficiency may lead to impaired host heme production, affecting the ability of hookworms to sustain infection. This discovery has potential ramifications for how humans are treated for hookworm infection. Traditionally, patients infected with hookworms are at risk for becoming anemic and are given iron supplements as part of their treatment. Results from this study, however, suggest that this treatment could actually be allowing the parasite to thrive in its host (48).

Correspondingly, another nematode that may lack heme biosynthetic enzymes is *Brugia malayi,* a filarial nematode that infects one hundred and fifty million people

worldwide (49). Genomic studies of two other filarial nematodes suggest the possibility that *Brugia malayi* requires heme for reproduction and development via hemoproteins that catalyze hormone biosynthesis. It appears that *B. malayi* may be another natural heme auxotroph and it likely obtains heme either from its host or possibly from *Wolbachia*, an endosymbiotic bacterium. *Wolbachia* contains all but one of the heme biosynthetic enzymes and is most likely responsible for supplying heme to *B. malayi.* In human trial studies, *B. malayi* infected patients have been successfully treated using antibiotics that target *Wolbachia.* Targeting the heme uptake pathway in *Brugia malayi* is another potential pharmaceutical target as it appears that the survival and growth of this organism requires heme (49).

The field of mammalian heme transport has only recently begun to identify genes involved in this process. Two mammalian mitochondrial porphyrin transporters have been identified, one of which also appears to transport heme (10,12). Additional advances in mammalian heme transport have revealed two genes responsible for heme export in hematopoietic stem cells (11,50). One of the mammalian mitochondrial porphyrin transporters discovered is ATP-binding cassette transporter ABCB6, which locates to the outer mitochondrial membrane and is required for mitochondrial porphyrin uptake (12). Experiments conducted in two mouse models demonstrated that the expression of this protein directly responded to intracellular amounts of heme. Mice treated to enhance splenic erythropoiesis showed an increase in *Abcb6* mRNA. Abcg2, also known as the breast cancer resistance gene (Bcrp1), is a member of the ATP-binding cassette family of drug transporters that transports drugs and toxins from cells (51). In *Abcg2* knockout mice

that have higher levels of protoporphyrin IX, mRNA levels of *Abcb6* were significantly higher in the bone marrow, liver, kidney, and testis (12). Heme biosynthesis, erythroid differentiation, and intracellular levels of protoporphyrins were shown to directly influence levels of murine ABCB6 *in vivo.* In K562, SAOS-2, and MEL cells, overexpression of *Abcb6* had a six to thirteen fold increase in accumulation of protoporphryn IX, an increase blocked by the heme synthesis inhibitor, succinyl acetone, suggesting that increasing *Abcb6* expression increased heme biosynthesis. ABCB6 associates with the outer mitochondrial membrane and is thought to transfer coproporphyrinogen III to the enzyme coproporphyrinogen oxidase which resides on the inner mitochondrial membrane to facilitate heme biosynthesis (12).

Another mitochondrial porphyrin transporter recently characterized is 2-oxoglutarate carrier (OGC), an inner mitochondrial membrane protein known to facilitate uptake of 2-oxoglutarate into the mitochondria (10). The studies involved the use of two fluorescent porphyrin derivatives PdTCPP and PdTAPP. PdTCPP accumulated in the mitochondria and co-localized with the mitochondrial marker, Mito Tracker. OGC was identified as the protein bound to PdTCPP by using latex bead technique and mass spectrometry. It was then shown that 2-oxoglutarate uptake into the mitochondria was inhibited by porphyrin derivatives. Uptake of PdTCPP into the mitochondria was prevented by 2-oxoglutarate, while hemin and two heme precursors, protoporphyrin IX and coproporphyrin III, inhibited 2-oxoglutarate uptake into the mitochondria. This carrier protein is conserved in yeast and humans and may play a role in the accumulation of heme and heme precursors in the mitochondria

(10). In spite of these promising results, there are a few caveats in this study. One is the primary role of the synthetic fluorescent derivative PdTCPP, a compound whose physiological properties are not clear. Another question to address is why heme would be transported *into* the mitochondria. And finally, in each of these papers (10,12), the authors used the commercially available oxidized planar conjugated macrocycle, coproporphyrin III, rather than the physiologically relevant substrate coproporphyrinogen III, a reduced nonplanar porphyrin (52).

Until recently, no proteins that specifically transported heme had been identified. Within the last two years, two mammalian heme transporters were identified: the feline leukemia virus receptor (FLCVR) and the ABC transporter (ABCG2) (11,50). Both of these apical membrane proteins were shown to facilitate the export of heme from hematopoietic stem cells, preventing toxic levels of heme from accumulating. Preventing expression of FLVCR by siRNA causes a decrease in the number of colony-forming unit erythrocyte cells, induces apoptosis, and subsequently prevents erythroid differentiation. Expression of FLVCR in CaCO-2 cells reduces cellular heme concentration during intestinal cell differentiation (31). While the role of FLVCR in intestinal and liver tissues remains unclear, ABCG2 localizes on the apical membrane of duodenal enterocytes and in other regions of the gastrointestinal tract. The definitive function of these proteins as heme exporters in the intestine remains to be explored.

Currently, the protein or proteins responsible for dietary heme absorption into intestinal cells are unknown. While it was recently reported that the long-sought heme carrier protein had been identified and subsequently named HCP1, a group

several months later reported that HCP1 is a proton–coupled folate transporter and that it could not be more than a poor heme transporter (53). Therefore, the search for a mammalian gene or genes that facilitate intestinal heme uptake continues.

Techniques used to localize heme

There have been many techniques developed to localize heme within cells, many of which involve fluorescent (14,15), histochemical (7,8), and radiolabeling approaches (16). Recently, heme trafficking was observed in live cells for the first time in the cattle tick*, Boophilus microplus* (15). This parasitic heme auxotroph relies on the blood of its host for nutrients and can ingest quantities of blood up to one hundred times its own body mass. During the ensuing breakdown of hemoglobin, potentially toxic levels of heme are generated and sequestered into a recently described organelle called the hemosome (54). To observe heme trafficking within the cell, researchers used the fluorescent heme analog Palladium–mesoporphyrin IX (Pd-mP) (15). Pd-mP fluoresces red when bound to proteins and green when free. This enabled the researchers to determine when and where the heme analog was bound to proteins in live digest cells of the *B. microplus*. Pulse-chase experiments revealed the heme analog was bound to protein while being trafficked from digestive vesicles through the cytoplasm, and then transported into the hemosome. When the analog was present in the cytoplasm, it fluoresced red and this fluorescence intensified at the edge of the hemosome (15).

Histochemical staining methods have also previously been established to pinpoint heme localization in mammalian tissue using the chromogenic substrate, 3-

3'diaminobenzidine (DAB) (7). This technique exploits the oxidative property of the ferrous iron (FeII) within the tetrapyrrole ring. The iron in the center of heme reacts with hydrogen peroxide to generate hydroxyl radicals as shown in the following equations:

$Fe^{2+} + H_2O_2 \rightarrow Fe^{3+} + {}^{\cdot}OH + OH^-$

$Fe^{3+} + H_2O_2 \rightarrow Fe^{2+} + {}^{\cdot}OOH + H^+$

Hydrogen peroxide oxidizes FeII of heme to ferric iron (FeIII), a hydroxyl radical, and a hydroxyl anion. FeIII is then reduced back to iron II by another round of reaction with hydrogen peroxide to a FeII peroxide radical, and a proton. The hydroxyl radicals oxidize DAB, producing a localized red-brown product.

This technique has been used to study heme absorption in the rat (7) and dog (8) models. Rats, like many eukaryotes, synthesize heme in addition to taking it up from their diet. The purpose of this study was to follow the pathway of intestinal heme uptake in the rat duodenum. Electron micrographs showed that heme was released from hemoglobin in the intestinal lumen, then entered the mucosal cells through the apical pits. The heme was next observed in the apical tubules, and was finally observed in the secondary lysosomes of the apical and supranuclear regions of the cell (7). However, the experimental conditions differed greatly from normal heme uptake by the rat. The heme was administered surgically to the animals in quantities sufficiently large enough see a reaction product generated by DAB (7). The canine model has been used to demonstrate that the sub-cellular route of

hemoglobin–iron absorption through intestinal epithelial cells is different from the absorption of inorganic iron (8). Studies using this model concluded that endocytosis appeared to play a major role in heme absorption, offering insight into a possible route of hemoglobin-iron.

In the current study, we have established a whole animal heme staining methodology using the natural heme auxotroph, *C. elegans*. By carefully controlling the heme levels in the growth medium of this nematode, we characterized heme localization in mutants which show aberrant growth in response to heme and in wild type N2 worms. To our knowledge, this is the first time heme localization has been characterized in a whole animal. This established protocol will enable us to further our current understanding of eukaryotic heme trafficking by providing a conceptual framework for approaches such as Raman confocal microscopy.

Chapter 2: Materials and Methods

Worm strains and growth medium

The N2 wild-type strain of *C. elegans* was used for all experiments except where indicated. Mutant worm strains IQ911, IQ1068, IQ938, IQ731, IQ828 were obtained by Dr. Anita Rao. These mutants are capable of surviving in high levels of heme (> 800 μM) that are otherwise toxic to wild-type worms. The worms were grown in axenic CeHR medium that was modified (mCeHR) to eliminate all sources of exogenously added heme under aerobic conditions at 20°C in tissue culture flasks. Synchronized L1 larvae were added to mCeHR axenic liquid medium at a population level of ~1500 worms/mL and grown in designated heme concentrations until they reached the mid-L4 larval stage, at which point they were fixed, permeabilized, and stained for heme.

Worm permeabilization and fixation for light microscopy

N2 worms were grown to the gravid stage in growth medium containing 20 μM hemin chloride (Frontier Scientific, Logan, UT) and bleached [1.1 % Clorox bleach (sodium hypochlorite)/0.55 M NaOH] to harvest the eggs. Eggs were washed 2-3 times with M9 buffer (86 mM NaCl (Fisher, #S271-43), 42mM Na_2HPO_4 (Fisher, #S774), 22mM KH_2PO_4 (Acros, #42420-5000), 1mM $MgSO_4$ $7H_2O$ (Acros, #423905000)) and synchronized by hatching overnight in M9 buffer solution.

When the worms reached the L4 larval stage, they were harvested for fixation and permeabilization. The L4 worms were washed three times with M9 buffer

solution and then incubated in the M9 buffer solution for 1 to 3 h to empty gut contents. Afterwards, the animals were transferred to a 1.5 mL microfuge tube, allowed to settle for 10 min, washed with 1.0 mL distilled water and allowed to settle for an additional 10 min.

The permeabilization method was modified from a previously published method (55). After the supernatant of the settled worms was aspirated, the microfuge tube was placed on ice. One ml of ice-cold paraformaldehyde solution [50 % Modified Ruvkin's Witches Brew: (160 mM Potassium Chloride (Acros, #42409-0010), 40 mM NaCl (Fisher Scientific, #S271-3), 20 mM EGTA-Sodium salt, 10 mM spermidine HCl (MP Biomedicals, #194542), 30 mM Pipes pH 7.4 (Acros, 17261-1000), 50 % methanol (Fisher, #A412-4), 40 % distilled water, 2 % paraformaldehyde (Sigma, #41678-0010)] was added to the centrifuge tube containing the worms and the contents were mixed gently so to avoid damaging the worm tissues. The centrifuge tube was incubated at 4°C for 35 min with occasional mixing. Following this step, the worms were allowed to settle and washed twice with 1.0 mL Tris Triton Buffer [100 mM Tris HCl pH7.4 (Acros, #14050-0025), 1.0 % Triton X-100 (Acros, #422435-5000), and 1.0 mM EDTA (Acros, # 40997-5000)]. The animals were then incubated at room temperature in 1.0 mL of 1 % β-mercaptoethanol (Acros, #12547-1000) in TTB for 15 min at eight RPM on a platform shaker (Platform shaker by Barnstead Thermolyne). The worms were washed once with 1X borate buffer [25mM H_3BO_3, 12.5mM NaOH)] and allowed to settle. One mL of 10 mM DL-1,4 Dithiothreitol 99 % (Acros, #16568-0050) in 0.9X borate buffer (22.5 mM H_3BO_3, 11.25mM NaOH) was added to the tube of worms. The centrifuge tube was rotated

on the Labquake shaker for 15 min at room temperature. The worms were then rinsed five times with distilled water and stored overnight at 4°C in PBS buffer [13.7 mM NaCl (Fisher # 5271-3), 0.27 mM KCl (Acros, #42409-0010), 0.43 mM Na_2 HPO_4 (Acros, # 42437-5000), 0.14 mM KH_2PO_4 (Acros, # 42420-5000) that had been deoxygenated with N_2 gas. These fixed and permeabilized worms were stained the following day.

Pre-staining solution to eliminate oxygen radicals

To eliminate oxygen radicals that can oxidize the staining chemical, 97 % 3-3'diaminobenzidine tetrahydrochloride, 97 % (Acros, #112090050) solutions used in all experiments (unless otherwise noted) were deoxygenated by flushing with nitrogen gas for 15 - 20 min just prior to staining. Fixed and permeabilized worms were rinsed three times with deoxygenated potassium phosphate buffer (pH 7.4) (4.05 mM K_2HPO_4 and 0.95 mM KH_2PO_4) incubated in the dark at 37°C for 2 hr in a solution containing 0.2 % bovine liver catalase (Sigma, # C-1345) (56), 0.04 % bovine liver superoxide dismutase from bovine liver (Sigma, #S-186) in potassium phosphate buffer, pH 7.4. The worms were then rinsed twice with deoxygenated 0.06 M Tris HCl buffer (pH 8.0-8.2).

Heme staining for light microscopy

A solution of 0.15 % DAB in 0.06 M Tris HCl (pH 8.0-8.2) was added to all samples. Then, H_2O_2 (Sigma, #H1009) was added to each staining group for a final concentration of 0.06 %. Control samples were incubated with DAB in the absence

of H_2O_2. All samples were incubated for 30 min under deoxygenated conditions and rinsed three times with deoxygenated, distilled H_2O. The worms were mounted on 0.1 %– 0.2 % agar (Fisher Bioreagents, # BP26411) beds, prepared on glass slides and photographed using a Leica DMIRE2 DIC microscope fitted with a Retiga 1300 cooled 12-bit CCD camera and imaged with SIMPLEPCI version 5.2 Software (Compix, Inc.).

Heme staining analysis

The control groups of worms were always evaluated before the experimental groups to ensure that staining in the controls was sufficiently minimal to permit analysis. Staining in the controls typically varied slightly in intensity, but the final reported percentage of staining in the controls included all variations of staining intensity. The majority of control groups in the following experiments had ~ 10 % staining. One or two slides containing worms from the control group was evaluated. Each slide contained ~300-500 worms. The entire slide was examined to determine the percent of worms stained out of the whole group. The experimental groups were evaluated in the same manner as the control group. While there was some variation in staining intensities in the experimental samples, final conclusions were based upon the degree to which > 70 % of the worms stained.

Worms were examined and photographed using bright field light microscopy. Differential interference contrast (DIC) microscopy was not used in the majority of the heme staining experiments due to difficulties capturing heme staining in photomicrographs.

DAPI staining

An unsynchronized population of wild-type worms were grown at 20 μM heme and fixed by the chemical fixation method described in this section. The worms were then stained with a 1 μg/ml DAPI solution (Sigma, #32670) for 10 min at room temperature.

Worm fixation and permeabilization using microwave fixation

Due to poor preservation of tissue structure integrity, the fixation and permeabilization method used for light microscopy could not be used for electron microscopy. Instead, a *C. elegans* fixation and permeabilization protocol was modified from a previously described method (57) (communication, Dr. David Hall at the Albert Einstein College of Medicine). Wild–type N2 worms were grown in axenic mCeHR medium containing 80 μM heme. When the worms reached mid-L4 stage, they were rinsed once with M9 buffer solution and incubated in the M9 buffer solution for 1 to 3 h to clear gut contents. The M9 buffer solution was changed once every hour. Worms were washed once with distilled H_2O and placed on ice for transport to the University of Maryland Laboratory of Biological Ultrastructure (LBU) for microwave fixation (Pelco 3440 Laboratory Microwave oven and Pelco 3420 Microwave Load Cooler). At the LBU, the worms were rinsed three times with fixative solution [1.0 % glutaraldehyde **(**Acros**,** # 233280250**),** 0.05 M sucrose (Acros, #220900010), and 0.1 M Hepes, pH 7.4. (Sigma, #H-3375)] and placed into one well of a three-well glass chamber slide. The hotspots of the microwave were detected prior to each microwave fixation so that the worms were microwaved within

the hotspots. The hotspots were predetermined using a probe placed over the grid located on the floor of the microwave oven. The probe contained individual bulbs that aligned with each grid box. When the microwave was turned on, the bulbs that flashed red indicated the areas of the grid that contained the hotspots. These hotspots varied from use to use. The glass chamber slide was placed into an ice bath (a 150 mm Petri dish full of crushed ice). The chamber well containing the worms was placed directly over a previously determined hotspot. The worms were microwaved at 70°C at full power for 1.5 min ON and for 2 min OFF for a total of five cycles. After each cycle, the glutaraldehyde fixative solution and the ice bath were changed. This process was repeated five times. Once these five cycles were completed, the worms were microwaved at the same temperature and power settings for 1 min for three cycles with a 4 min recovery period. The total time exposed to microwave energy was 10.5 min. The animals were then incubated at 37°C for 1 h in the 0.2 % catalase and 0.04 % superoxide dismutase solution in 5 mM phosphate buffer, pH 7.4., described earlier. The worms were rinsed twice with 0.06 M Tris HCl (pH 8.0-8.2) and divided into control and staining groups.

Heme staining for electron microscopy

A solution of 0.15 % 3-3'diaminobenzidene, 0.06 M Tris HCl (pH 8.0-8.2), and 0.06 % H_2O_2 was used to stain worms for 30 min at room temperature under deoxygenated conditions. The control group was incubated in the absence of hydrogen peroxide. After staining, the worms were rinsed three times with deoxygenated, distilled water. The worms were then incubated in a counterstaining and fixative solution of 0.1 %

osmium tetroxide (EMS, 19140) for 33 min at room temperature. The worms were then washed five times with deoxygenated, distilled water and embedded in epoxy resin.

Worm embedding

All materials used for embedding were purchased from Electron Microscopy Services (EMS, Fort Washington, PA) unless otherwise noted. Agarose beds were made by pouring 3.0 - 4.0 mL of 3.0 % Low Melt Preparative Grade Agarose (BioRad, 162-0019) into 60 mm petri dishes. Approximately four to twelve worms were arranged side by side on top of the first layer of the solidified agarose and then covered with another 3.0 to 4.0 mL of agarose, so the worms were sandwiched between the two beds. The Petri dishes were stored overnight at 4.0°C with a few drops of water on top of the agar beds, to prevent the agar from drying out.

The next morning, each group of worms were cut out of the bed with a razor blade to a size that would fit into the tips of the embedding molds (Pelco International, #105). Each piece of agarose contained four to twelve worms that could be placed coronally or sagitally into the tips of the mold. The pieces of the agarose beds could not be bigger than the mold nor smaller than the tip of a Pasteur pipette. The worm samples in agarose were dehydrated by placing them in 25 mL glass bottles and incubating for 5 min in each of the following ethanol grades: 30 %, 50 %, 75 %, and 95 %. For the final ethanol dehydration step, the worms were incubated in 100 % ethanol three times, each time for 10 min. Further dehydration steps were necessary, and they were carried out in propylene oxide (PO) (1,2-

Epoxypropane, Methyloxirane, (#20412). All PO steps were conducted using only glass or polypropylene equipment, as PO is highly reactive. The agarose pieces were incubated in PO three times, each time for 10 min. Worms were incubated in a 2:1 ratio of PO:resin mixture for 2 to 3 h on a vertical rotator (Barnstead Thermolyne) at room temperature. The resin mixture contained 45.0 % Embed 812 (#14900), 30.0 % Dodecenyl Succinic Anhydride (DDSA) (#13710), 25.0 % Nadic Methyl Anhydride (Methyl-5-Norbornene-2,3-Dicarboxylic Anhydride) (#19000), 1.5 % DMP-30 (2,4,6-Tri (dimethylaminomethyl) phenol, (#13600). Resin was made fresh for each experiment and stored under vacuum in a room temperature desiccator. The worm sections were then incubated in a 1:2 PO:resin solution overnight at room temperature on the vertical rotator. Approximately 15 h later, the agarose pieces were removed from the PO: resin mixture and placed into resin for 3 h at room temperature. During this 3 h incubation period, the resin was changed twice. Following the second change of resin, the agarose pieces were positioned at the tip of the embedding mold with the worms either coronally or sagitally placed. Small pieces of paper with the assigned sample code, which differentiated the samples from one another, were placed into the molds. Resin was poured into the embedding molds, making sure the worms remained correctly aligned at the tip. The molds were cured for 3 days at 60°C, removed from the oven, and allowed to cool for at least half a day.

Thin sectioning

At the end of the embedding process the worms were thin-sectioned for electron microscopy (EM) on an American Optical Ultracut microtome with a glass knife

(Ultramicrotomy grade glass (# 71012) generated by a glass knife cutter (LKB 7800B Knifemaker). Water boats to catch the thin sections, were made with plastic water boats (#71007) and sealed to the glass knife with clear nail polish (#72180). A chloroform solution was used to flatten the sections and a Zerostat Ion Gun (153) was used to minimize static electricity. The sections were approximately 60 nm – 90 nm thick, and were placed on coated 375–mesh copper grids. The samples on the grids were counterstained with lead citrate (#17800) and uranyl acetate (#22400). The uranyl acetate solution was made by dissolving 0.2 g dry uranyl acetate in 10 mL of distilled H_2O. This solution was stirred overnight at room temperature. The lead citrate solution was made by dissolving 0.03 g in 10 mL H_2O and adding 0.1 mL 10 M NaOH, shaking vigorously by hand for 5 min and storing overnight at 4°C. Prior to staining, these solutions were centrifuged for 10 min at room temperature to remove any particulate matter. Electron micrographs were taken under the direction of Mr. Tim Maugel, with a Zeiss EM10 Transmission Electron Microscope at the LBU.

Chapter 3 Characterization of heme localization in wild-type worms using light microscopy

Summary

Heme is a tetrapyrrole essential to life for many organisms. In most of these organisms, heme is both synthesized in a well-conserved eight-step pathway, as well as absorbed from the diet. Heme uptake has been studied morphologically since the 1960's, but most of the animals used for those studies were heme synthesis prototrophs. We use the nematode *Caenorhabditis elegans* as the model organism of choice to study heme transport because we recently discovered that it does not synthesize heme but utilizes heme from diet (13). Thus, the *in situ* study of heme uptake in this animal will provide a better understanding of how heme transport is mediated in eukaryotes without interference from endogenous heme sources. Here, we show that, by using a DAB staining technique and light microscopy, *C. elegans* stains robustly for heme, revealing a direct correlation between histochemical heme staining and the level of nutritious heme administered exogenously in the growth media. Wild-type worms that were grown at 1.5 μM, 4.0 μM, 20 μM, 40 μM, and 100 μM heme showed a proportional increase in the intensity of heme staining. Our systematic standardization of the methodology of heme staining builds upon earlier work, and establishes an *in vivo* approach to directly visualize heme in an intact whole animal. This new method is a useful starting point for the study of *in situ* heme trafficking in *C. elegans.*

Rationale

This research project was designed to cytologically localize and characterize heme staining in *C. elegans* using microscopy. The overall research goal of our research group is to discover the molecules controlling heme transport pathways in *C. elegans.* *C. elegans* is a free-living nematode that does not synthesize heme, but requires exogenous heme for incorporation into hemoproteins (13). We hypothesize that specific intracellular pathways must exist for heme transport because heme is an essential molecule that cannot simply diffuse into, within and between cells due to its hydrophobicity and cytotoxicity. *C. elegans* is an ideal organism to address questions pertaining to heme transport for a number of reasons. First, *C. elegans* does not contain any of the well-conserved genes required for heme biosynthesis, and thus we have complete control over heme transport in the animal. Second, *C elegans* is translucent, proving to be an ideal system to localize heme within cells and organs in the intact animal. Third, *C. elegans* is a well-established genetic model with invariant somatic cell number. It has been used for genetic and cell biological studies for more than thirty-five years (58).

Complete control of heme transport is difficult to attain in eukaryotic organisms that synthesize heme (13). Establishing a protocol for *in situ* heme labeling using the chromogenic substrate 3-3' diaminobenzidine (DAB) will allow us to gain a better understanding of where hemes are localized and transported *in vivo* in *C. elegans*, a natural heme auxotroph. Histochemical staining with DAB exploits the peroxidase activity of heme, and has been used extensively for the last forty years to

study heme uptake and trafficking in various model organisms. When hydrogen peroxide is added as a second substrate, the iron in the center of the heme ring reacts with the hydrogen peroxide, releasing oxygen radicals. These oxygen radicals oxidize DAB and produce a localized brown/red reaction product (17). Previous heme labeling microscopy studies in other organisms used artificially elevated heme levels in organ slices. The studies described herein, however, localize histochemical heme *in situ* in intact *C. elegans* under normal and varying levels of physiological heme concentrations.

Results

Our goal for this project was to cytologically localize heme in whole animals using *C. elegans*. This manner of cytologically localizing heme in worms has not been reported in the literature. As a starting point, we conducted our first staining experiment by attempting to use a procedure established by Graham and Karnovsky (17). This study described a new histochemical staining technique using DAB, to study horseradish peroxidase absorption in the mammalian kidney, using the rat model. This method involved incubating the worms for 10 min in a DAB-saturated staining solution in 0.05M Tris HCl buffer, pH 7.6. Two groups of worms were tested with this staining procedure. The first group of worms had been fixed and permeabilized two days earlier as described in the Materials and Methods section (59). The second group of worms was fixed and permeabilized by the same method, on the same day. Within 10 min of the staining reaction, the worms in the control samples (minus H_2O_2), permeabilized two days earlier, showed non-specific staining.

However, no staining appeared in either the control group (minus H_2O_2) or the experimental group (plus H_2O_2) of the worms that had been fixed on the same day. After these results, we decided to try to modify the protocol as described by Simionescu *et al*., that was used for one of the first EM studies for heme uptake in mammalian intestine (60). This modification called for a staining incubation period of 60 min and for the DAB Tris-HCl buffer solution to have a pH of 8.0. This experiment produced significant levels of non-specific staining. We then decided to try to establish our own heme staining methodology.

Addition of catalase to pre-incubation solution

Our first heme staining experiment, based on a previously published method (17) produced inconclusive results. There was no difference in staining between the worms in the control samples and worms in the experimental samples. Our first thought was that endogenous hydrogen peroxide could be oxidizing DAB, producing non-specific staining in the control samples. To eliminate this endogenous hydrogen peroxide, we incubated the worms, post-fixation, in a 0.2 % catalase (CAT) solution in 5 mM phosphate buffer for 30 min at 37°C, as described in the Materials and Methods section. CAT is the enzymatic catalyst in the chemical reaction below:

$$2\ H_2O_2 \xrightarrow{CAT} 2\ H_2O + O_2$$

While there was still significant non-specific staining, we noticed for the first time that gravid worms contained the majority of the non-specific staining. Staining was reduced in the samples by ~ 40 % (Figure 3).

Figure 3: Addition of CAT to eradicate peroxide radicals.

A mixed population of N2 worms grown at 20 μM heme in mCeHR medium was permeabilized as described in Materials and Methods and stored overnight in PBS at 4°C. After 15 h, the worms were incubated in 5 mM potassium phosphate buffer, pH 7.4 containing 0.2 % CAT for 30 min at 37°C, in the dark. The staining reaction was carried out for 30 min at room temperature. Staining in the control samples incubated with CAT by ~ 40 %. This experiment was performed one time, and each micrograph is a representative image. Scale bar = 100 μm.

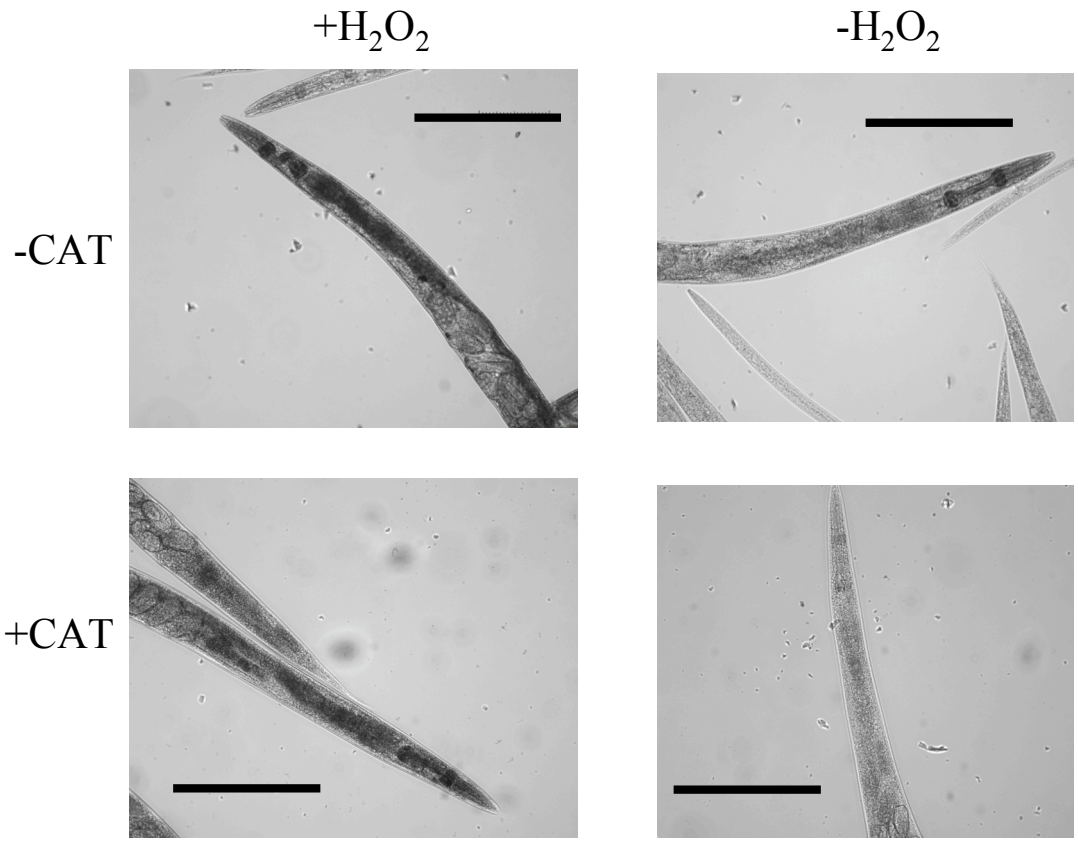
+H2O2
-H2O2
-CAT
+CAT

While we achieved a significant improvement in the non-specific staining of the controls by adding the CAT step, we felt it was necessary to further standardize the staining procedure. We tested three additional concentrations of CAT for a longer period of time to see if there would be any differences in the staining of our control samples. In addition to the 0.2 % used originally, we tried 0.02 %, 0.1 %, 0.2 % and 1.0 % of CAT in 5mM phosphate buffer, pH 7.4 for 2 h at 37°C. No differences were detected in staining of the controls between these four concentrations. The experimental samples of gravid worms in each of the different concentrations of CAT stained only 30 - 40 % greater than the gravid worms in the control samples. We again noted that the gravid worms in the control samples had non-specific staining while the non-gravid adults and larval worms in the control samples had very little, if any, non-specific staining. Experiments conducted later confirmed that larval worms consistently had less non-specific staining than gravid worms.

Addition of SOD to pre-incubation solution.

Although we significantly reduced the non-specific staining in our control samples by incubating the worms with CAT, we added another modification. Since endogenous H_2O_2 is generated by the reaction catalyzed by the enzyme superoxide dismutase (SOD), we rationalized that pre-incubation with SOD would help reduce the non-specific staining observed in the control samples. SOD catalyzes the following reaction in conjunction with CAT.

$$O_2^- + O_2^- + 2H^+ \xrightarrow{SOD} O_2 + H_2O_2$$

$$2H_2O_2 \xrightarrow{CAT} 2H_2O + O_2$$

Surprisingly, > 90 % of the worms in the experimental group stained for heme, while < 5 % of the control group revealed non-specific staining. The staining observed in the experimental group was throughout the entire worm and the staining intensity was uniform, as shown in Figure 4. No other distinct staining patterns were observed.

Heme staining unsynchronized worms grown at 20 μM and 100 μM heme

The addition of SOD and CAT to our protocol showed promising results by reducing the non-specific staining. We then decided to try and compare staining levels between two mixed, unsynchronized populations of worms grown at 100 μM and 20 μM heme. The worms were fixed, permeabilized, and 15 h later, pre-incubated with 0.2 % SOD and 0.2 % CAT in 5 mM phosphate buffer, pH 7.4. The worms were then stained for heme with 0.15 % DAB in 0.06 M Tris HCl, pH 8.0. The results from this experiment are shown in Table 1. During this experiment there were no differences in staining between the gravid worms, and their embryos, in the control and experimental groups. DAPI staining of the nucleus in these worms, described in Materials and Methods, revealed that >75 % of the eggs and 90 % of worms were permeabilized. Control samples of worms grown at 20 μM and 100 μM heme did not differ in their staining intensity. Importantly, worms grown at 100 μM heme from the experimental group had significantly darker and more intense heme staining than experimental worms grown at 20 μM heme. This experiment indicated that worms grown in different concentrations of heme display differences in the intensity of heme staining. These results also indicated that gravid worms have significantly higher levels of non-specific staining, independent of the addition of H_2O_2.

Figure 4: Addition of SOD to erradicate oxygen radicals.

A mixed population of wild-type worms was grown in 20 μM hemin and their F_1 progeny were synchronized as described in Materials and Methods. The L1 larvae were inoculated into 20 μM heme in mCeHR medium. At the L4 larval stage the worms were harvested, fixed, permeabilized, and stored overnight at room temperature. The following morning the worms were incubated in a pre-incubation solution of 0.2 % CAT and 0.2 % SOD in 5 mM phosphate buffer for 1 h. The worms were subsequently stained for heme. Less than 5.0 % of the control samples stained while > 90 % of the experimental samples stained. This experiment was performed one time and each micrograph is a representative image. Scale bar = 100 μm.

+H_2O_2

-H_2O_2

Table 1: Larval worms have significantly less non-specific staining than gravid worms.

The majority of worms in the control group that stained were gravid. Approximately 5 % of the larvae in the control samples had non-specific staining. Greater than 85 % of the stained worms in the experimental group, however, stained specifically for heme.

[Heme]	Control		Experimental	
	Gravids	Larvae	Gravids	Larvae
20μM	~40 %	5 %	> 90 %	> 85 %
100μM	~40 %	5 %	> 90 %	> 90 %

To eliminate the problem of non-specific staining in gravid worms, we conducted our next experiment using only larvae. This experiment was also designed to further test the possibility of differential heme staining of worms grown at different heme concentrations.

Heme staining in synchronized L4 larvae at 20 μM and 100 μM heme

To test whether worms that were grown in higher heme concentrations stained more intensely than worms grown at lower heme levels, synchronized L1 larvae were grown in mCeHR medium in 20 μM and 100 μM heme. The results are shown in Table 2 and Figure 5. Worms grown in 100 μM heme stained approximately 2- 3 fold more intensely than worms grown in 20 μM heme as shown in Figure 5.

Synchronized L4 larvae grown at 1.5 μM, 4 μM, 20 μM, and 40 μM heme were stained for heme using deoxygenated conditions.

While we significantly improved the specific staining with the addition of SOD and CAT, and using only larval worms, we observed that worms in the control group would begin to stain during the rinsing process, post staining. Because staining results from the oxidation of DAB, it was possible that oxygenation of the rinsing solution was causing this experimental artifact. We decided to go one step further and stain the worms, now under deoxygenated conditions, using the apparatus shown in Figure 6. The results are shown in Table 3 and Figure 7. As might have been predicted, worms grown in 40 μM heme stained the most intensely. The worms grown in 20 μM heme concentrations stained slightly more intensely than the L4 larvae grown at 4 μM heme.

Table 2: Synchronized L4 larvae exhibit specific heme staining.

Approximately 5 % of the 100 μM larvae revealed staining throughout the body in the control group. Worms grown at 100 μM heme showed > 95 % heme staining in the experimental group and > 80 % of those worms showed uniform staining throughout the body. Worms grown at 20 μM showed staining in > 80 % of the experimental group and this staining was throughout their body. Less than 5 % of the 20 μM worms stained in the control group.

[Heme]	Control	Experimental
20 μM	< 5 %	> 95 %
100 μM	~ 5 %	> 80 %

Figure 5: Synchronized L4 larvae grown at 20 μM and 100 μM heme exhibit differences in heme staining intensity.

Synchronized L1 larvae obtained from N2 worms grown in 20 μM heme were inoculated into mCeHR medium containing either 20 μM or 100 μM heme. When these larvae reached the L4 stage, the worms were fixed, permeabilized, and stored overnight as described in Materials and Methods. Approximately 15 h later, the worms were stained for heme. The experimental samples from the worms grown at 100 μM heme stained 2 -3 fold more intensely than the worms grown at 20 μM heme. This experiment was performed one time and each micrograph is a representative image. Scale bar = 100 μm.

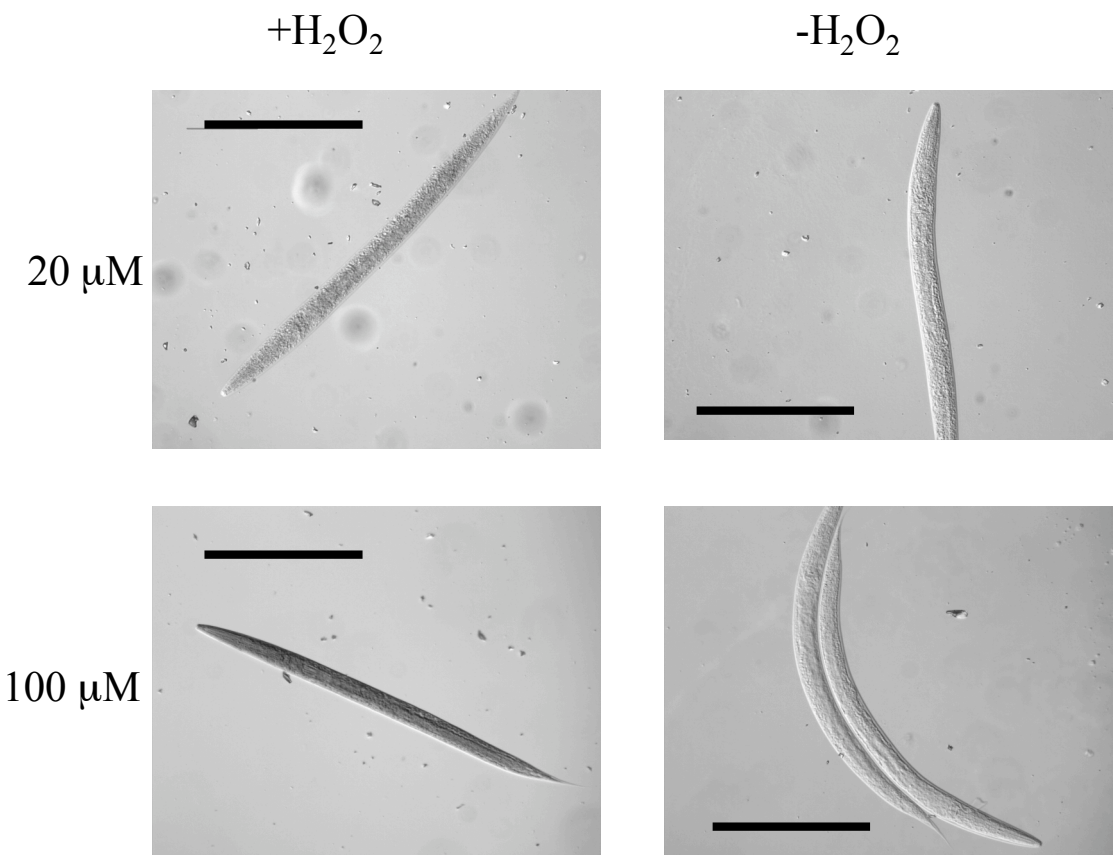
+H2O2
-H2O2
20 μM
100 μM

Figure 6: Experimental apparatus for deoxygenation of worm samples.
Each of the worm samples were contained in a plastic test tube fitted with a rubber septum. The needle of the apparatus was the source of N2 gas for the test tubes containing the samples. A separate needle was inserted through the rubber septum of the test tubes, allowing the oxygen and nitrogen to escape.

Needle attachment for sample tubes fitted with a rubber septum (see image below)

Tubing connected to nitrogen gas tank

Needle attachment (through which the N_2 gas flows)

Needle allows oxygen to escape

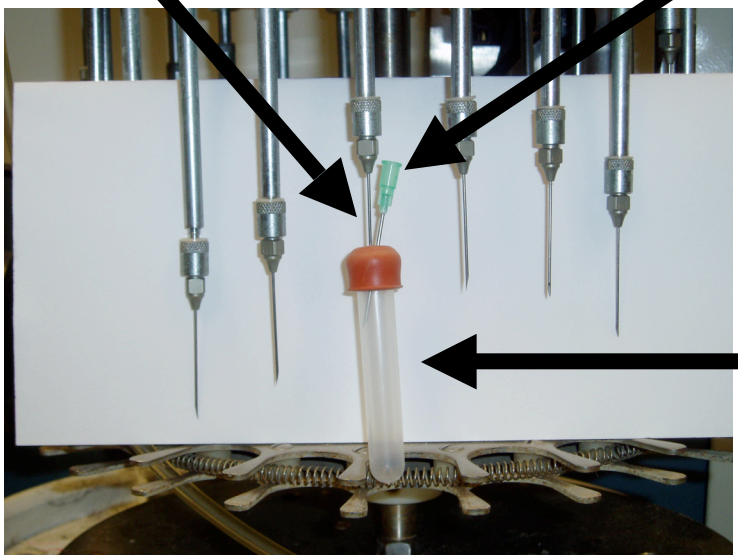

Test tube containing sample

Table 3: Syncronized L4 larvae exhibit significant levels of specific heme staining when stained under deoxygenated conditions.

Synchronized L1 larvae from wild-type worms grown in mCeHR medium and 20 μM heme were inoculated in mCeHR medium, supplemented with 1.5 μM, 4 μM, 20 μM, and 40 μM heme until they reached the L4 stage. The synchronized L4s were fixed, permeabilized, and stored overnight as described in Materials and Methods. Approximately 15 h later, the worms were stained for heme under deoxygenated conditions described in Materials and Methods. All experimental samples had > 80 % specific heme staining.

[heme]	**Percent of worms that stained within each group**	
	Control	Experimental
1.5 μM	0 %	> 80 %
4.0 μM	0 %	> 80 %
20 μM	~ 5 %	> 80 %
40 μM	15 %	~ 90 %

Figure 7: Synchronized L4 larvae grown at 1.5 μM, 4 μM, 20 μM, and 40 μM heme and stained for heme under deoxygenated conditions.

Wild-type worms were grown in 20 μM heme and mCeHR medium. Their eggs were harvested by bleaching and hatched overnight in M9 buffer as described in Materials and Methods. The synchronized L1 larvae were then inoculated in mCeHR medium supplemented with 1.5 μM, 4 μM, 20 μM, and 40 μM heme and allowed to develop to the L4 stage. The synchronized L4 worms were fixed, permeabilized, and stored overnight as described in Materials and Methods. The larvae grown at 40 μM heme had the most intense staining of all the experimental samples, while the difference in heme staining intensity between 1.5 μM, 4 μM, and 20 μM was not significant. This experiment was performed one time and each micrograph is a representative image. Scale bar = 100 μm.

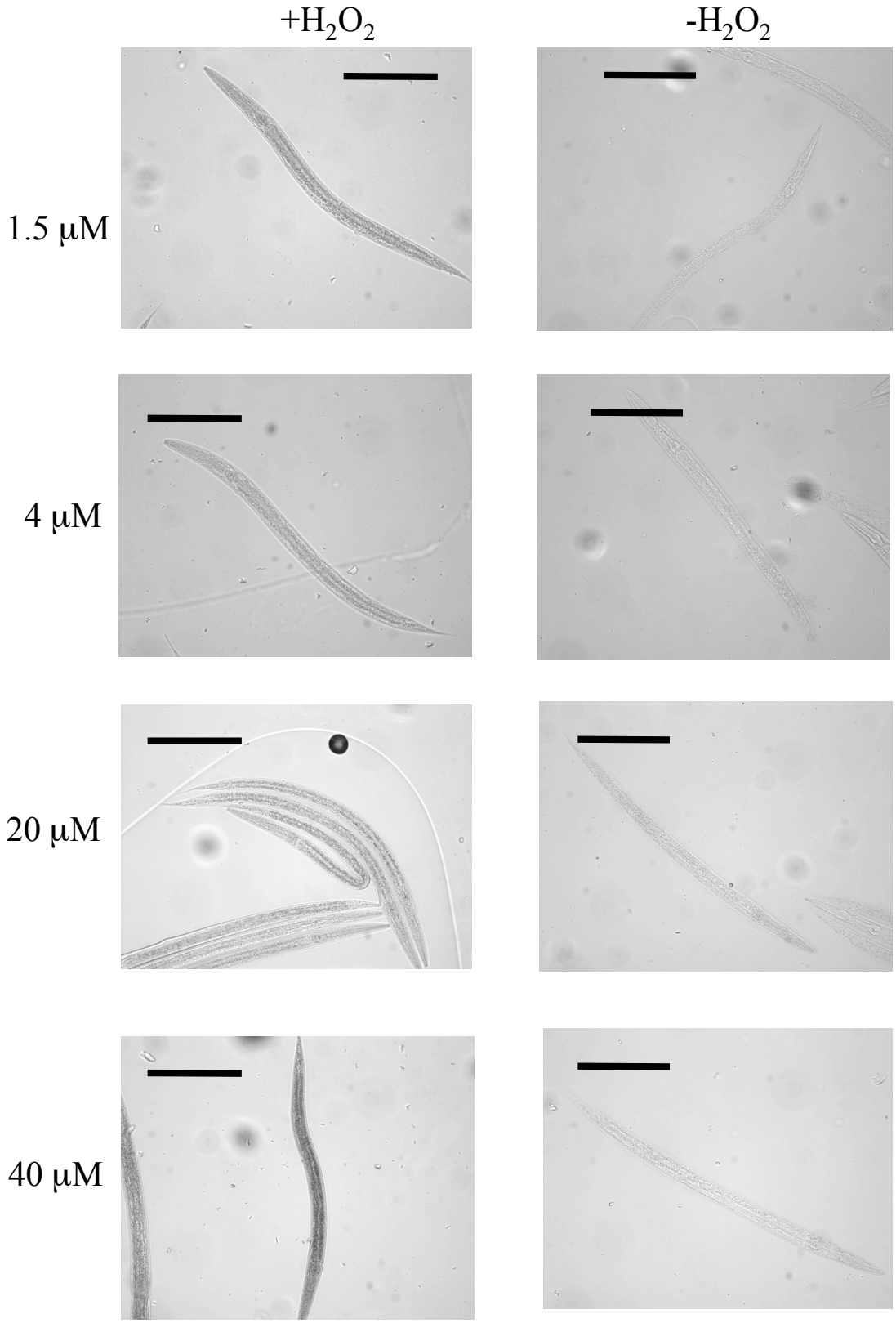
+H2O2
-H2O2
1.5 μM
4 μM
20 μM
40 μM

The experimental samples from the worms grown at 1.5 μM heme exhibited staining that was not significantly different from staining of experimental worm samples from 4 μM and 20 μM heme. The difference in staining intensity between 4 μM, and 20 μM larvae was not as great as the difference between either of those groups and 40 μM (Figure 7).

Mixed population of worms grown at 1.5 μM, 4 μM, 20 μM, and 40 μM heme

We were able to drastically reduce the non-specific staining in our control samples by incubating the worms in a CAT/SOD solution and staining the worms under deoxygenated conditions. We then decided to stain mixed populations of worms to determine if deoxygenated conditions would reduce the non-specific staining in gravids in the control groups. Mixed populations of worms were grown in 1.5 μM, 4 μM, 20 μM, or 40 μM heme, then fixed, permeabilized, and stored overnight as described in Materials and Methods. The worms were then stained for heme as described in Materials and Methods.

As shown in Table 4, > 80.0 % of gravid worms in the control group stained, and the larvae in this group showed minimal levels of non-specific staining. Based on these results and results from previous experiments, we decided to use synchronized non-gravid worms for future staining. To determine the optimal time for analysis, the stained worms were analyzed either immediately or the following day. Optimal results were obtained when samples were analyzed the same day the staining procedure was performed.

Table 4: Differences in specific heme staining between larval and gravid worms at 1.5 μM, 4 μM, 20 μM, and 40 μM heme.

Mixed populations of worms were grown in mCeHR medium and 1.5 μM, 4 μM, 20 μM, or 40 μM heme. They were permeabilized, fixed, and stained for heme as described in Materials and Methods. For gravid worms, there was no difference in staining between experimental and control groups. Larval worms, however, exhibited significant levels of specific heme staining.

	Percentage of worms that stained within each sample			
[heme]	**Control**		**Experimental**	
	Gravids	Larvae	Gravids	Larvae
1.5 μM	> 80 %	< 1 %	100 %	~ 80 %
4 μM	100 %	~ 5 %	100 %	~ 70 %
20 μM	> 90 %	< 1 %	100 %	~ 60 %
40 μM	> 90 %	< 10 %	100 %	~ 80 %

Standardization of necessary SOD concentration

In order to determine the optimal staining conditions, we used varying levels of SOD (0.02 %, 0.06 %, 0.1 %, 0.15 % and 0.2 %). While we were trying to establish the minimum concentration of SOD required to minimize staining in our control samples, there were additional results from this experiment. We were able to determine that a concentration of 0.02 % SOD sufficiently minimized non-specific staining; less than 10 % of the worms in the control samples stained. We also observed, for the first time, distinct, punctate intestinal heme staining in the experimental groups. Two punctate staining patterns were observed. Punctate staining seen outside the intestine (Figure 8A and 8B) or in the intestine (Figure 8C and 8D).

One other observation we noted throughout all of our heme staining experiments was that the majority of heme staining was concentrated in the anterior half (first 5 pairs) of intestinal cells (Figure 9).

Figure 8: Intestinal punctate staining.

Wild-type worms were grown in 20 μM heme in axenic mCeHR medium. Their progeny was synchronized and grown in mCeHR medium containing 4 μM heme. The worms were harvested at the mid-L4 stage, fixed, permeabilized, and stored overnight as described in Materials and Methods. Approximately 15 -18 h later, the worms were stained for heme as described in Materials and Methods. Two punctate heme staining patterns were observed. One pattern showed heme staining outside the intestine (A and B), while the other pattern exhibited heme staining within the intestinal cells (C and D). The arrows within each of these figures indicate the punctate staining. This experiment was performed one time and each micrograph is a representative image. **A, C, E** scale bar = 100 μm. **B and D** scale bar = 25μm.

A + H_2O_2

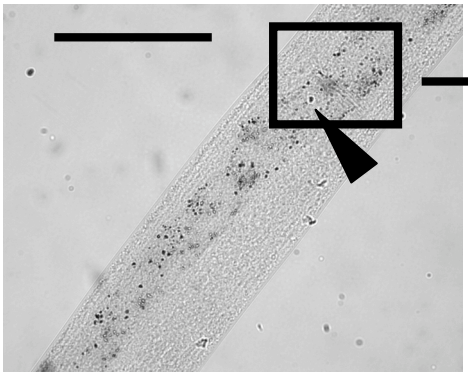

B

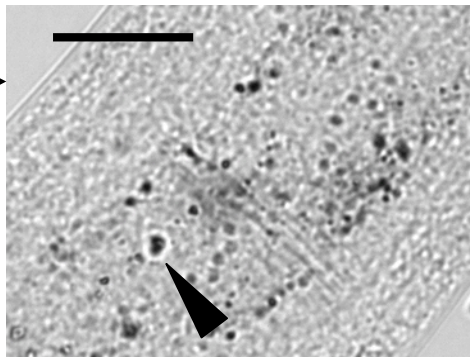

C + H_2O_2

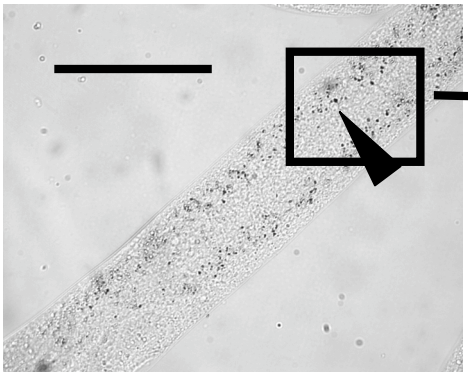

D

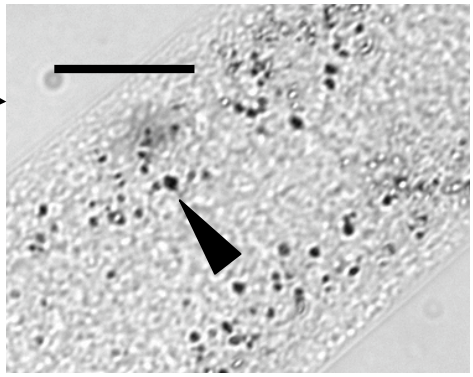

E

-H_2O_2

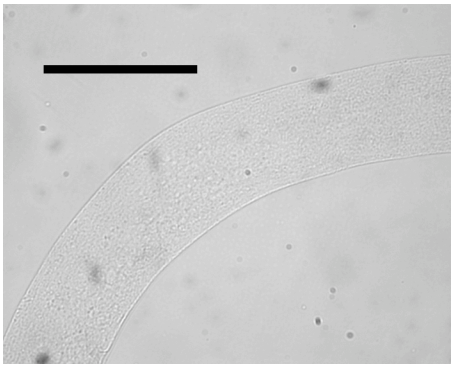

Figure 9: Heme absorption in intestinal cells.

Larval worms were grown in 1.5 μM heme, harvested, fixed, and permeabilized as described in Materials and Methods. Approximately 15 h later, these worms were stained for heme as described in Materials and Methods. The heme staining signal was most intense in the anterior intestinal cells and decreases in intensity until there is almost no detectable signal in the posterior intestinal cells. Scale bar = 100 μm.

+H_2O_2

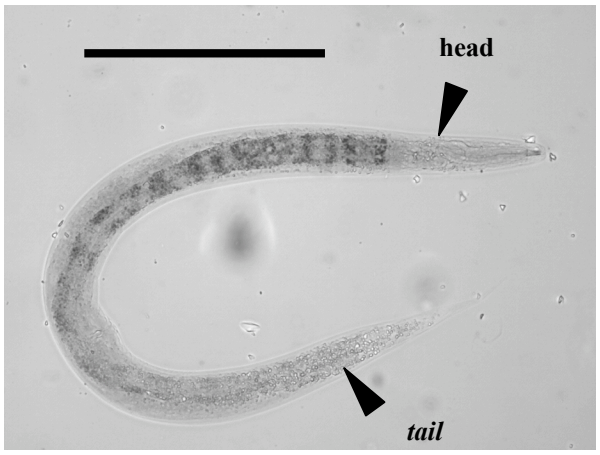

-H_2O_2

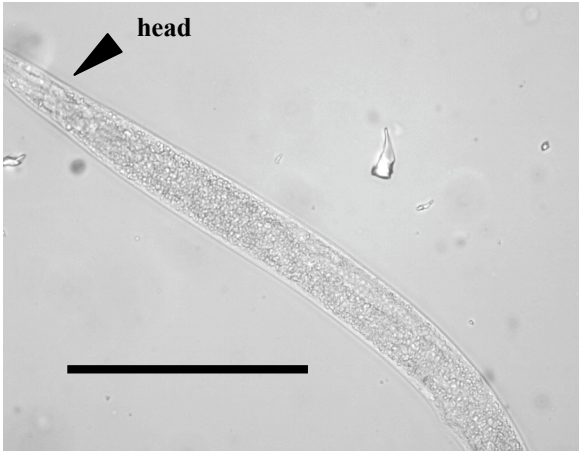

Chapter 4: Application of new heme staining technique

Summary

We have developed and optimized a methodology to histochemically detect *in situ* heme under normal physiological conditions in *C. elegans.* We applied this heme staining protocol in three capacities: to evaluate qualitative differences in heme levels and localization between the mutant and wild-type worms, to explore the possibility that the maternal heme effect in *C. elegans* could be visualized by staining, and to continue heme staining studies of wild-type worms at the electron microscopy (EM) level. Our research group identified 13 strains of *C. elegans* mutant in heme homeostasis and 5 of these mutant strains were selected for this heme staining study. We show that all but one of the five mutants selected exhibit less intense heme staining than wild-type. We then tested possible heme staining differences caused by the maternal heme effect. A maternal effect occurs when the offspring phenotype is due solely to substances directly passed to the offspring from the mother, whether the substances are mRNA, proteins, or other molecules, such as heme. Results from this experiment show that *C. elegans* progeny of wild-type worms grown in different heme concentrations stain differently for heme. Finally, to more precisely locate heme within individual cells, we applied our heme staining technique to EM experiments in order to characterize heme staining at the ultrastructure level in *C. elegans.* In each of these experiments, we experienced issues with non-specific staining in our control samples, preventing us from drawing any insightful

conclusions about heme localization in *C. elegans* at the EM level. However, these results also indicated that heme staining *C. elegans* at the level of the light microscope provides a starting point from which to examine heme uptake and localization at the ultrastructure level.

Rationale

We hypothesize that heme homeostasis is mediated by specific molecules. To identify the genetic determinants of heme, a forward genetic screen conducted in our research group obtained thirteen strains of worms mutated in heme homeostasis. Phenotypically, these worms are capable of surviving in 800 μM or 1 mM concentrations of heme, levels that are toxic to wild-type worms. In principle, these mutants could differ from wild-type worms in that the heme transport pathway(s) either transport less heme into intestinal cells, sequester heme more efficiently, or more rapidly detoxify heme. In order to further understand heme transport in *C. elegans*, we utilized our heme staining technique and compared differences in heme levels between the mutant and wild-type worms grown at low concentrations of heme.

A maternal effect occurs when the source of an offspring phenotype is due solely to substances including mRNA, androgens or other compounds that are passed on to the offspring by the mother. This phenomenon has been characterized in wasps, birds, and humans (61-64) and most importantly, in *C. elegans,* involving proteins such as phosphatase, isomerase, and CDK (65,66). *C. elegans* requires heme for growth and development but is unable to synthesize it. The fact that transferring

maternal substances to the progeny is vital to their embryonic growth and development led us to postulate that maternal heme might also be passed on to progeny. Furthermore, while *C. elegans* is a non-parasitic nematode, there are several known parasitic nematodes that are also heme auxotrophs. It is possible that the maternal proteins responsible for transferring heme to the embryos could potentially be drug targets to limit these parasitic infections (13). Unpublished data have shown that when F_1 larvae obtained from P_0 worms that were grown in low (4 μM), optimal (20 μM), and high (500 μM) heme were inoculated into medium containing no added heme, F_1 progeny of the worms grown at 4 μM heme growth arrested at the L3 larval stage, while the F_1 progeny of the worms grown at 500 μM growth arrested as early adults. These results suggested that heme levels available to the mother affected the subsequent growth and development of her offspring. We therefore examined differences in heme staining intensity and localization between the progeny of worms grown at 4 μM, 20 μM, and 500 μM heme.

Previous work conducted to study eukaryotic heme uptake and localization at the ultrastructure level used abnormal, non-physiological conditions of heme-loading in organisms that synthesize heme. One of these studies designed to characterize heme uptake in the rat duodenum at the EM level used heme administered to rats as hemoglobin or hemin chloride in highly concentrated quantities through an intragastric tube (7). Administration of high quantities of hemoglobin/hemin chloride is abnormal as well as non-physiological. We have standardized a technique to stain heme in whole animals, under normal growth conditions of heme, using the heme

auxotroph *C. elegans*. It is our goal to apply this heme staining technique in EM experiments in order to characterize heme localization in wild-type worms. Using *C. elegans* allows us to completely control the concentration of heme available to the animal. Additionally, the location of every one of its 959 somatic cells is the same in every animal, allowing us to precisely identify heme localization in each cell. Furthermore, the entire worm has been sectioned and the images are available online at www.wormimage.org to use as a reference for characterizing where cellular heme is located.

Results

Worms mutated in heme homeostasis display differential heme staining as compared to wild-type worms.

An unpublished study was conducted using random EMS-based mutagenesis in *C. elegans* to identify mutants resistant to toxic heme levels (800 μM). Dr. Anita Rao isolated 13 mutants which belong to 5 complementation groups (Table 5). The rationale for characterizing these mutants for heme staining is that disruption in heme homeostasis by either heme transport or heme sequestration would lead to survival under toxic heme levels. Thus, the logical extension for our studies would be to examine how much and where heme localized in these mutants at the level of the light microscope. For this experiment, we analyzed one mutant from each complementation group, as indicated in Table 5. The experiment was conducted twice and the results are summarized in Tables 6 and 7. There was no staining observed in worms from the control groups (Table 6). Only 50 % of the worms in any of the experimental groups revealed heme staining. All of the heme staining was

punctate, and restricted to the first 5 pairs of intestinal cells. Mutant worms IQ731, IQ938, IQ828, IQ911 had less intense heme staining than wild-type. However, IQ911 revealed the lowest intensity in the punctate staining than any of the other mutants (Figure 10). In contrast to the other four mutants, IQ1068 revealed an increase in staining intensity compared to wild-type worms.

Progeny obtained from worms grown at different heme levels stain differentially for heme.

Wild-type worms were grown for at least two generations in 4 μM, 20 μM, and 500 μM heme. Their eggs were harvested, synchronized overnight in M9 buffer. The following morning, the synchronized larvae were inoculated into mCeHR medium with no added heme, and allowed to grow for six days. On day 6, there were no visible gravid worms by microscopic examination in each of the three groups. However, there were notable differences in their developmental stage. F_1 progeny from 4 μM heme were growth arrested at the L3 stage while F_1 progeny from the 500 μM heme were arrested at the early adult stage. F_1 progeny from 20 μM growth arrested at the early L4 stage. The difference in growth rates of these worms is summarized in Table 8. The progeny were then histochemically stained for heme as described in the Materials and Methods section. No staining was observed in any of the samples in the control groups. The larvae that stained the most intensely for heme were from the progeny of worms grown at 500 μM heme (Figure 11). The larvae from worms grown at 20 μM heme stained less than half as intensely as the progeny of the worms grown at 500 μM heme. Heme staining in larvae obtained from worms grown at 4 μM heme was barely detectable, as shown in Figure 11.

Table 5: Complementation groups of heme-resistant mutant worms.

The thirteen mutants resistant to high heme are grouped in 5 complementation groups [courtesy of Dr. A. Rao and B. Le]. Mutants selected to analyze by heme staining are highlighted with a gray box.

Complementation groups	Mutants in each complementation group				
I	IQ911				
II	IQ828				
III	IQ728	IQ938	IQ968		
IV	IQ921	IQ718	IQ731		
V	IQ1058	IQ1048	IQ1068d	IQ1031	IQ1068

Table 6: Percent of specific heme staining in wild-type worms and worms mutated in heme homeostasis.

N2, IQ938, IQ731, IQ911, IQ828 and IQ1068 worms were grown in mCeHR medium with 4 μM heme. F_1 embryos were harvested, synchronized, and inoculated at 4 μM heme. When they reached the mid-L4 stage, they were stained for heme as described in Materials and Methods. There was no staining in worms from the control groups. In worms from the experimental groups, only 50 % of the worms showed heme staining, which was punctate.

Worm strain	Control	Experimental
N2	0 %	50 %
IQ938	0 %	50 %
IQ731	0 %	50 %
IQ911	0 %	50 %
IQ828	0 %	50 %
IQ1068	0 %	50 %

Table 7: Heme resistant mutants reveal differential heme staining.

The mutant worm strains IQ828, IQ938, and IQ938 all exhibited staining that was slightly less intense than wild-type, while IQ911 heme staining was significantly less intense than wild-type. Only one strain, IQ1068, exhibited heme staining that was more intense than wild-type.

Mutant complementation group	Relative intensity compared between wild-type and mutant
I	N2 >> IQ911
II	N2 ≥ IQ828
III	N2 ≥ IQ938
IV	N2 ≥ IQ731
V	N2 ≤ IQ1068

Figure 10: Heme staining wild-type, IQ731, IQ911, IQ828, IQ1068, and IQ938 strains grown at 4 μM heme.

Wild-type, and mutant strains IQ731, IQ911, IQ828, IQ1068, and IQ938 were grown in 4 μM heme in mCeHR medium for two generations. Their eggs were harvested and hatched overnight in M9 buffer. The synchronized L1 larvae were inoculated into 4 μM heme in mCeHR medium. When the worms reached the mid-L4 stage, they were fixed, permeabilized, and stored overnight as described in the Materials and Methods section. Approximately 15 – 18 h later, the worms were stained for heme using the protocol described in the Materials and Methods section. This experiment was performed two times and each micrograph is a representative image. Scale bar = 100μm .

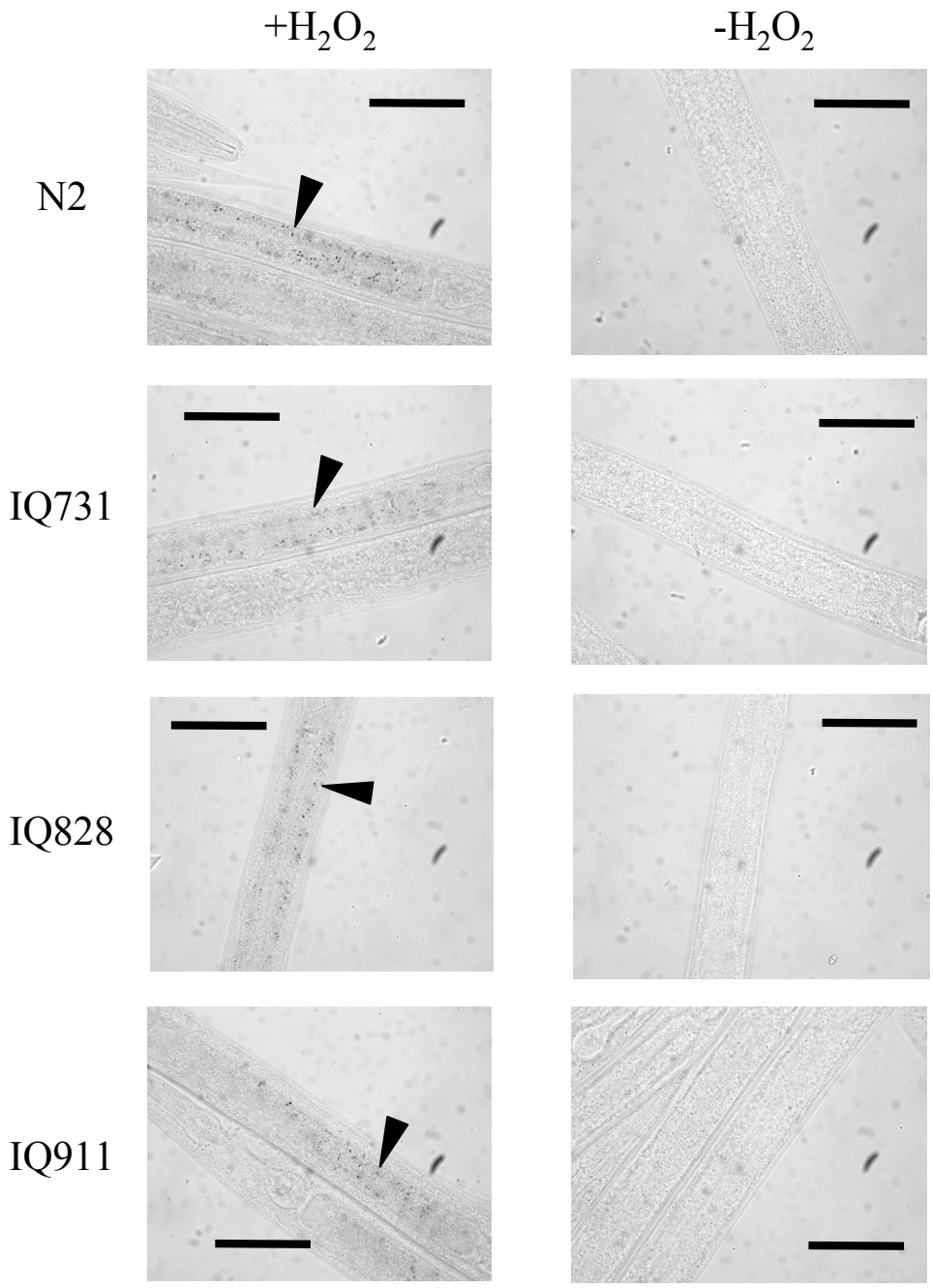
+H2O2
-H2O2
N2
IQ731
IQ828
IQ911

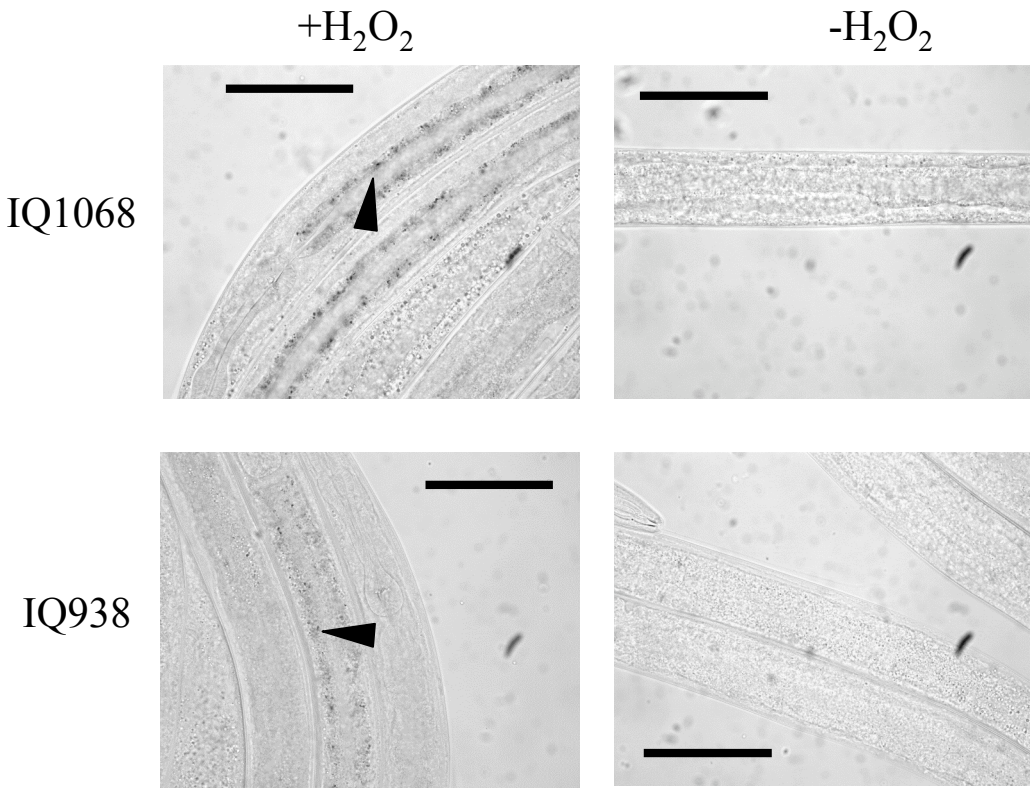
+H2O2
-H2O2
IQ1068
IQ938

Table 8: Maternal heme effect on growth rates of progeny obtained from parental worms grown at different heme concentrations.

F_1 progeny of worms grown at 4 μM, 20μM, and 500μM heme were grown in mCeHR medium with no added heme for six days. After 24 h, the F_1 progeny of worms grown at 4 μM heme had reached the L3 larval stage, the stage at which their growth was arrested. F_1 progeny of worms grown at 20 μM heme reached the mid-L4 stage after 49 h, after which they developed no further. The F_1 progeny of worms grown at 500 μM heme reached the early adult stage after 94 h and did not ever become gravid. ND = not detected.

[Heme] available to P_0 worms	**Time required for F_1 progeny to reach growth stages**			
	L3	**Early L4**	**Mid-L4**	**Early adult**
4μM	24 h	ND	ND	ND
20μM	24 h	40 h	49 h	ND
500μM	24 h	40 h	49 h	94 h

Figure 11: Progeny obtained from worms grown at different heme levels reveal a maternal heme effect.

Wild-type worms were grown for at least two generations in 4 μM, 20 μM, or 500 μM heme. Gravid worms were bleached, and their eggs were harvested and synchronized overnight in M9 buffer as described in Materials and Methods. Synchronized L1 larvae were inoculated into separate flasks of mCeHR medium with no added heme. After 6 days, the worms were harvested, fixed permeabilized, and stained as described in Materials and Methods. Heme staining in larvae obtained from worms grown at 4 μM heme was barely detectable. The larvae from worms grown at 20 μM heme stained less than half as intensely as the progeny of the worms grown at 500 μM heme. The larvae that stained the most intensely for heme were from the progeny of worms grown at 500 μM heme. The arrow bars indicate heme staining. This experiment was performed five times and each micrograph is a representative image. Scale bar = 100 μm.

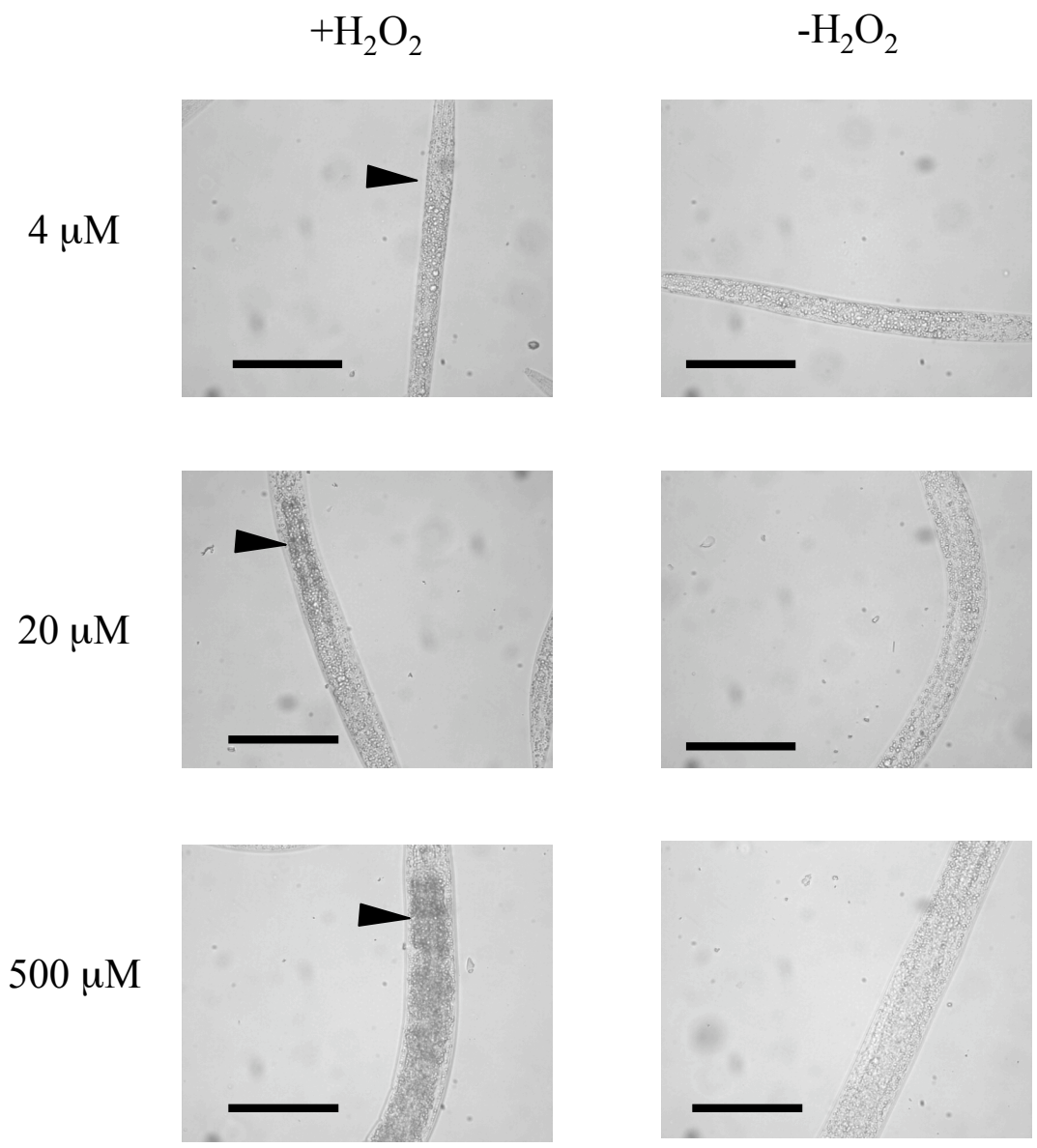
+H2O2
-H2O2
4 μM
20 μM
500 μM

Preliminary results of heme staining *C. elegans* at the ultrastructure level

For the electron microscopy studies we needed to modify the permeabilization and fixation protocol. *C. elegans* has a cuticle that is tough to penetrate by standard fixation and permeabilization methods. One permeabilization and fixation method available for *C. elegans* which allows for preservation of tissue integrity at the ultrastructure level is microwave fixation (57) Personal instructions were provided by Dr. David Hall, the Director of the Center for *C. elegans* Anatomy at the Albert Einstein College of Medicine. Microwave energy increases the rate at which fixative solutions penetrate the cuticle and subsequent underlying tissues. Additionally, this fixation method improves the penetration of resin, the embedding material, without any further exposure of the sample to the microwave energy (57). The previous chemical method provided sufficient permeabilization of the cuticle for heme staining analysis at the light microscopy level. However, preservation of the tissue structure was insufficient for analysis at the ultrastructural level (Figure 12).

We standardized the microwave fixation protocol in order to sufficiently preserve subcellular structures while simultaneously ensuring that heme staining can be observed at the ultrastructure level in *C. elegans*. Modifications were made to a previously published protocol (57) with personal communication from Dr. Hall.

DAB is the chromogenic substrate of choice because it has a distinct, localized electron dense reaction product. Furthermore, it has been shown that the reaction product of the compound may not be affected by the embedding process (17). It is important to note that we needed to re-establish the appropriate

concentration of DAB for microwave fixation because microwave fixation is not as penetrative as the chemical fixation that was used previously. Our first experiment tested three concentrations of DAB: 0.15 %, 0. 30 %, and 0.45 %. We stained synchronized L4 larvae that had been grown at 20 μM heme in mCeHR medium. The best results were obtained with worms with 0.15 % DAB, although there was very light staining in ~ 30.0 % of the worms from the control group. The two higher concentrations of DAB produced high staining (>50.0 %) in the control group. The tissue structure preservation, however, was superior to the previously used chemical fixation and permeabilization method as shown in Figure 12**.** We were satisfied with the preservation of tissue structure when observed under a light microscope, and proceeded with our EM studies.

Once we established the microwave fixation and heme staining protocols, we conducted a few electron microscopy studies to standardize the dehydration and embedding method given to us by Dr. Hall. As a first step, we decided to do the EM experiments with wild-type worms grown to mid-L4 stage in 80 μM heme. We chose to stain worms grown at 80 μM heme because we reasoned we would be able to see a greater heme staining signal without subjecting the worms to physiological toxic levels of heme. Mid-L4 larvae were harvested, fixed, and permeabilized by microwave fixation as described in the Materials and Methods section, and stained for heme using the DAB staining protocol previously standardized by us for light microscopy. This was followed by further fixation and counterstaining by osmium tetroxide, also described in Materials and Methods. The worms were embedded in

Figure 12: Comparison of microwave fixation to chemical fixation.
Synchronized wild-type L1 larvae were grown in 20 μM heme until they reached the mid-L4 stage. The L4 larvae were harvested, fixed, and permeabilized by microwave fixation as described in the Materials and Methods section. The same day, these worms were stained for heme. Permeabilization and fixation by microwave fixation showed substantially improved cellular structure preservation as compared to earlier studies using chemical fixation. This experiment was performed one time and each micrograph is a representative image. Scale bar = 100 μm

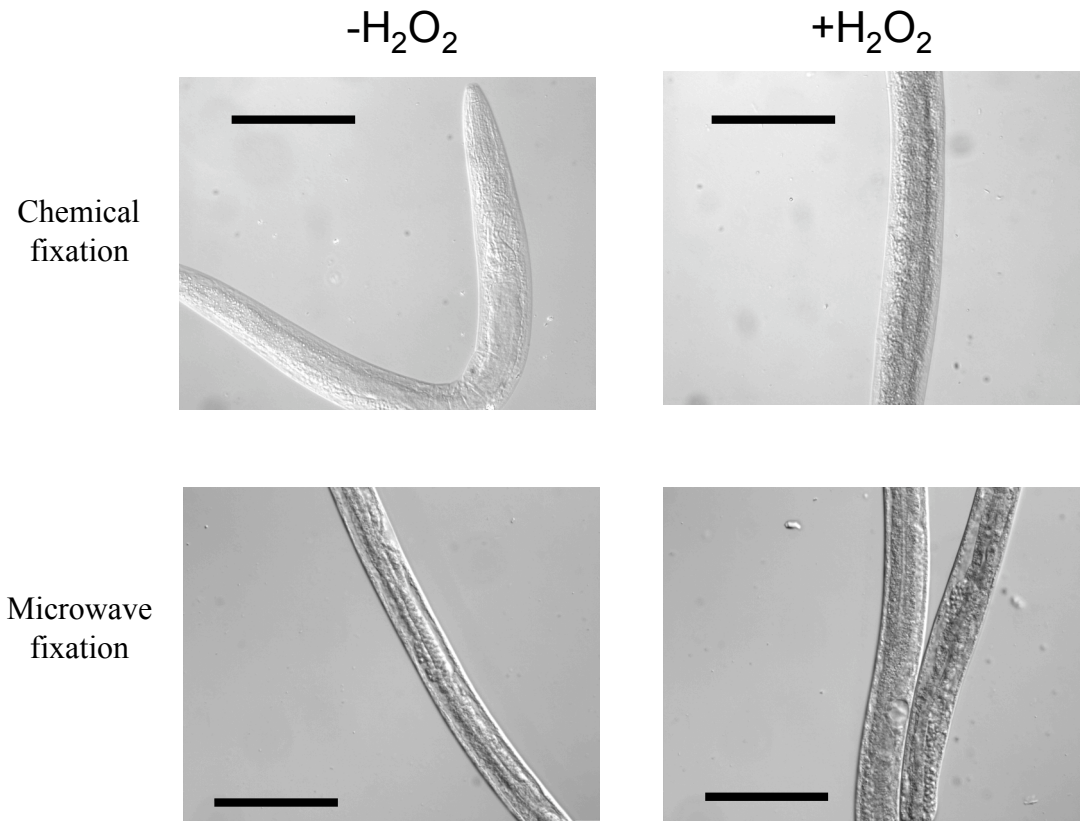
-H2O2
+H2O2
Chemical fixation
Microwave fixation

epoxy resin, thin–sectioned, placed on copper grids, and examined under EM, as described in the Materials and Methods section. Prior to the embedding process, worms are fixed and counterstained with osmium tetroxide. After the worms have been embedded and thin sectioned, the thin sections of tissue are further counterstained with lead citrate and uranyl acetate. To standardize counterstaining conditions of lead citrate and uranyl acetate, we based our first round of standardizations on the recommendation from Dr. Hall. We first tested multiple time points of lead citrate staining 1, 1.5 and 2 min and uranyl acetate time points at 10, 15, 20, and 25 min. There were no significant differences in electron dense spots between control and experimental samples. These results suggested the possibility that the counterstains may interfere with the visualization of heme. We decided to omit counterstaining with lead citrate because it was more likely to precipitate on the grid. To standardize the uranyl acetate counterstaining we incubated the grids for 0, 6, 8, and 10 min time points to determine the minimum counterstaining required to visualize the tissue using EM. After trying to standardize this round of counterstaining, we were still not seeing significant differences between control and experimental samples. We decided to counterstain using only osmium tetroxide to minimize the possibility of counterstaining precipitate.

Experiments were conducted with wild-type worms grown to the mid-L4 stage in 80 μM heme. The results from these two studies were inconclusive. When DAB is oxidized by hydrogen peroxide, it leaves a well-characterized, easily identifiable dark, electron dense precipitation product. Images from the two identical experiments conducted, revealed little difference in staining between worms from the

control and experimental samples.

Sections from nine different worms in the first experimental group were evaluated. The images taken were of the worm intestine. Present in these samples were storage granules that, because of their electron dense appearance, they were initially mistaken for possible heme containing vesicles, indicated by asterisks in Figure 13**.** However, upon examination of other *C. elegans* EM images, we determined that these vesicles were not heme. These structures are most likely to be gut granules described as having an electron dense appearance because of the various compounds they contain including carbohydrates, lipids and proteins (yolk granules), or concentrated waste products (www.wormatlas.org). These gut granules were present in both groups of worms incubated with DAB (controls and stained), as well as in a control group incubated in the absence of DAB.

In these experiments there were electron dense spots that caught our attention, but their presence in both control and stained groups led to the conclusion that we could not analyze the electron dense spots as heme staining. These spots varied in number, size and shape. A few sections from the experimental samples had as many as twelve dense spots, while others had only one or two. In the control samples, there was an average of 4-5 electron dense spots. Most of these spots were irregularly shaped and varied in size but sections from both experimental and control samples had an average number of about five irregularly shaped, electron dense spots (Figure 13).

Figure 13: Wild-type worms grown at 80 μM heme, histochemically stained for heme, and examined at the ultrastructural level.

Wild-type worms (P_0) were grown at 80 μM heme. Their eggs were harvested by bleaching, and synchronized overnight in M9 buffer. The following morning, the synchronized L1 larvae were inoculated into 80 μM heme in mCeHR medium. When the larvae reached the mid-L4 stage, they were processed for EM as described in the Electron Microscopy section of Materials and Methods. The arrows depict DAB staining observed in control and experimental samples. Asterisks depict gut granules. This experiment was performed three times and each micrograph is a representative image. **13A** scale bar = 6.67 μm. **13B** scale bar = 2.13 μm. **13C** scale bar = 3.3 μm.

A

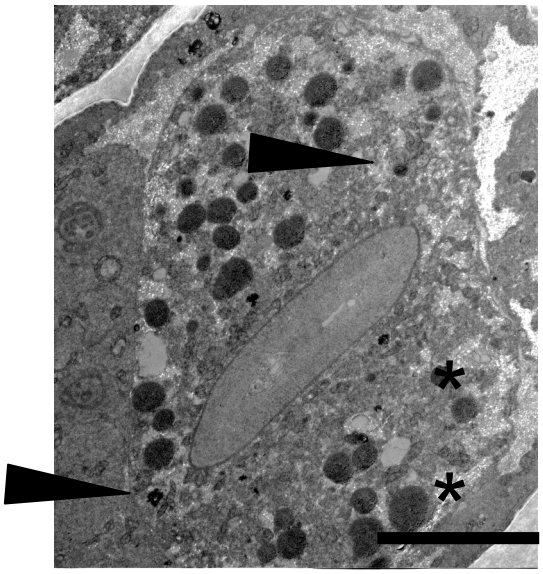

$-H_2O_2$

B

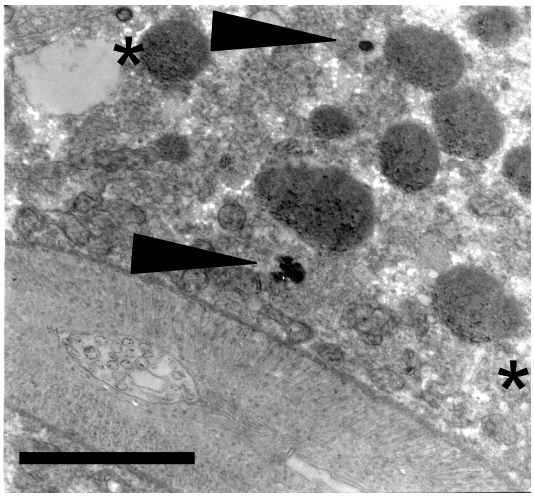

$-H_2O_2$

C

$+H_2O_2$

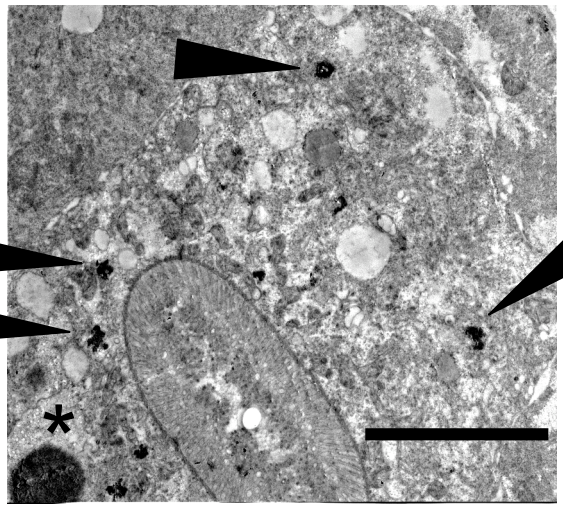

These electron microscopy experiments contained two different controls. The first control was incubated with DAB only, while the second control was incubated in the absence of DAB. Sections from the first control group contained 2-5 of the irregularly shaped, electron dense spots seen in the stained group of worms. Sections from worms incubated in the absence of DAB were examined and none of these sections had the irregularly shaped electron dense spots observed in the control samples incubated with DAB only ($-H_2O_2$). This suggested that there was non-specific DAB staining in our first (DAB only) control group. In conclusion of this series of experiments, comparisons between stained and control samples revealed areas of the cell with dark precipitate, presumably DAB staining. The precipitate spots were non-uniform in size, shape, and number per worm section (Figure 13) and could not be attributed to lead citrate or uranyl acetate because we did not counterstained the sections with these compounds.

Discussion

C. elegans is a natural heme auxotroph but relies on exogenously supplied dietary heme for metabolic functions. In the current study, we have established an *in situ* heme staining protocol for whole animals using *C. elegans.* While directly staining animal tissues for heme has been conducted for more than 20 years (7,8,54), to our knowledge, the ability to microscopically examine heme uptake and localization in an intact, genetically tractable animal under physiologic conditions of nutritional heme levels had not been accomplished. Additionally, we describe a method to stain worms for heme using a modified DAB method that has not been

reported previously.

Heme staining studies conducted on a heme auxotroph, the cattle tick *Boophilus microplus,* showed that this animal contains a specialized organelle called a "hemosome" for sequestration of large quantities of heme that this insect ingests (54). However, these studies were not corroborated with histochemical staining of heme in the intact tissue. Engorged ticks were dissected, and their midgut tissues, not their whole bodies, were stained for heme. Isolating and staining tissues from whole animals to study heme has been a standard practice for previous staining studies (7,8). Additional studies using digest cells of the tick and fluorescent porphyrin derivatives, of the tick the cattle tick showed heme transport in the cell (15). Unlike cattle ticks, *C. elegans* is translucent, making it ideal for cytological heme localization studies using light microscopy.

Establishing the methodology described herein took considerable time and effort as DAB, the chromogenic substrate used to localize heme, reacts with endogenous oxygen radicals to produce significant levels of staining in the samples from the control group with pre-incubation with SOD and CAT, we found that heme staining in *C. elegans* is does dependent (Figure 7). Furthermore, phylogenetically diverse nematodes, especially several species of parasitic nematodes, do not synthesize heme (13). This heme staining technique could provide valuable information on heme uptake, sequestration, and localization in nematodes.

Through the standardization process, we observed that eggs in gravid worms revealed considerable DAB reactive product in the control group. Furthermore, multiple staining experiments using gravid worms revealed no difference in staining

between gravid embryos of the control and experimental samples. Plausibly, , during during fixation and permeabilization steps, the embryo eggshell was sufficiently permeabilized to permit DAB entry (mw = 214 g/mol) but did not allow sufficient access to larger molecules, SOD (mw = 32.5 kDa for the dimer) and CAT (mw = 250 kDa for the tetramer). Based on these observations, we decided to focus on synchronized L4 larvae for future studies. We chose the L4 larval stage because this is the developmental stage at which the intestine of the worm is fully developed but embryogenesis has not yet begun, thus providing us with sufficient information regarding heme transport without confounding results due to variations in tissue permeabilization.

We also established a connection between the concentration of heme in the growth medium and the intensity of the heme staining observed in the worms. With the exception of worms grown at 1.5 μM heme, the higher the concentration of heme in the medium, the more intensely the worms stained for heme. The largest difference in staining intensities were observed between worms grown at 20 μM and 100 μM heme as well as between worms grown at 4 μM and 40 μM heme. Interestingly, in the second experiment, the group of worms grown in 1.5 μM heme stained more intensely than expected. Plausibly, under limiting heme conditions, heme uptake must be maximized to sustain normal growth and development. Indeed, unpublished microarray and qRT-PCR results suggest that a significant proportion of heme responsive genes (hrg's) are highly upregulated at 1.5 μM compared to 4 μM or 20 μM heme.

The differences in staining patterns between worms in earlier and worms of later experiments should also be addressed. Worms stained in earlier experiments exhibited uniform staining throughout their bodies. The punctate staining was observed in worms only in later experiments. There are several explanations for punctate staining, each involving the possible ways in which heme is absorbed into the intestinal cells. One possibility is that heme is absorbed by endocytosis. Heme contained within a vesicle formed by endocytosis, could cause the reaction that oxidizes DAB, therein, leaving localized punctate staining. Another explanation for the punctate staining involves a specialized vesicle into which heme is transported after it has been absorbed into the cell. Heme contained within this could also cause punctate staining.

There were two patterns of punctate staining: one which showed punctate staining outside the intestinal lumen, presumably concentrated within the intestinal cells, while the second pattern was punctate staining that appeared to be outside the intestinal cells. Although it is expected that heme will be located in both of these places, it is unclear why the punctate staining would remain segregated. Perhaps this is the limitation of using fixed versus live worms.

Another difference to note and further explore is the localization of punctate staining. Consistently, there was heavier staining in the anterior half of the intestine that faded gradually until there was virtually no detectable staining in the posterior cells. We speculate that the anterior intestinal cells may be the primary location for heme import and uptake in *C. elegans.* Consistent with this notion, the anterior portion of the intestine secrete digestive enzymes, take up nutrients, and have

membrane-bound organelles and vacuoles, while the posterior portions are active in energy storage, e.g., yolk and lipid vacuoles. Thus the differences we observe with heme staining throughout the intestine may reflect the difference in heme absorption intrinsic to *C. elegans* (Figure 9). Furthermore, corroborating evidence supporting this data was obtained using Raman confocal microscopy.

Differences in the histochemical heme staining among the mutants, as well as between the mutant and wild-type worms, suggest that these mutants may have differences in quantitative levels of heme. Each of these mutant strains of worms was selected as a representative strain from each of the 5 complementation groups. Whether these are qualitative differences in the precise location of the punctate staining cannot be addressed at the light microscopy level. One heme staining consistency between the mutant and wild-type worms was that the punctate staining in the mutants was consistently restricted to the first 5 pairs of cells in the anterior region of the intestine.

It is also important to note that even though worms from each of the five complementation groups were isolated based on heme resistance, IQ911 and IQ1068 showed opposite levels of heme staining compared to wild-type worms. IQ911 consistently showed less heme staining while IQ1068 showed more intense heme staining than wild-type. Furthermore, IQ938, IQ731, and IQ828 all showed heme staining that was slightly less than wild-type worms. It is currently not known how these animals are capable of surviving in concentrations of heme that are otherwise toxic to wild-type worms, but there are several conceivable explanations. One explanation, that would explain the less intense heme staining observed in IQ911,

IQ938, IQ728, and IQ828, is that these worm strains contain mutations in heme transporter machinery, resulting in import of less heme thus preventing the accumulation of toxic concentrations of intracellular heme. While IQ938, IQ731, and IQ828 all had growth rates similar to wild-type, the IQ911 strain consistently grew slower than wild-type by approximately 12 – 15 h. This observation is consistent with the notion that this strain reveals lower heme staining compared to wild-type worms. Conversely, strain IQ1068 showed slightly increased heme staining as compared to wild-type worms, possible because this mutant can detoxify or sequester heme differently than wild type. Taken together, future studies will be needed to address the biological mechanism for the observed differences in heme staining intensity in these mutants. Staining patterns and intensities in these mutants will be further characterized using heme analogs, RNA interference and heme reporter sensor strains.

C. elegans reveals a maternal effect for heme that is demonstrated by differences in growth and development, as well as in the intensity of histochemical heme staining. The differences in staining between the three experimental groups of worms were distinct. The likely sources of these differences are the levels of heme available to the parent and the amount of heme transported to the progeny during embryogenesis. Notably, the progeny with the highest level of heme, that reached the most advanced stage of development, never became gravid. Presumably, progeny from 500 μM worms had sufficient heme to undergo development to reproductive fitness, but initiation of embryogenesis must require heme levels greater than what was provided to them by their mothers. While it seems logical that the F_1 generation

could be supplied with sufficient heme to undergo embryogenesis, if the P_0 generation was grown at concentrations of heme > 500 μM, we found that this was not likely to be the case. Heme concentrations ≥ 800 μM are toxic to wild-type worms, and the worms growth arrest at the L3 stage (13). Future maternal heme experiments could be conducted with mutants to address whether or not the heme resistant mutations have any effect on the progeny phenotype.

Finally, we provide a framework and preliminary results for future ultrastructural heme localization studies in *C. elegans.* While there are a few problems that need to be first addressed and optimized prior to continuing EM studies, the implications for studying heme uptake and localization at the EM level using *C. elegans,* could have a significant impact in heme transport studies. There are numerous advantages to studying heme uptake in *C. elegans* at the ultrastructural level. First, *C. elegans* is a natural heme auxotroph that will have no endogenous heme to confound results. Another advantage is that the entire cell lineage of *C. elegans* has been mapped, and the location and number of all somatic cells does not vary between individual animals. Furthermore, there are thousands of unpublished EM images of *C. elegans* available on the World Wide Web, at www.wormimage.org. Many of these images contain labels identifying different cells and cellular structures, providing an invaluable tool for heme localization in specific cell types. Previously published studies of heme uptake at the electron microscopy level used animals that are heme prototrophs (7,8) and were conducted either under abnormal physiological conditions (7) or with radiolabeled heme (8) Our current protocol for heme staining in *C. elegans* provides a starting point from which

to pursue heme staining studies at the EM level. However, the conditions to observe heme at the ultrastructural level have to be optimized. Microwave fixation and heme staining using DAB produced good results at the light microscopy level. However, it is obvious that 30 % of staining in the control group, even though the staining was extremely light, confounded our results at the EM level. The following steps will need to be optimized: Establish a microwave fixation protocol that gives high permeabilization of worms without compromising the quality of the anatomical and morphological structure. This will permit the DAB to penetrate better at much lower concentration and for shorter incubation times such that worms from the control group give < 5 % visible staining. Levels of tissue preservation were also varied, so it is quite possible that reducing the time of exposure and controlling energy levels of the microwaves will improve the tissue structure at the ultrastructure level. This standardization will take a considerable amount of time because at each step the samples need to be examined at the ultrastructural level. Taken together, our studies suggest that individual parameters will have to be further optimized to adapt our histochemical *in situ* staining for heme at the light microscopy level to better preserve tissue and lower non-specific staining at the ultrastructural level for EM. Once these issues have been addressed, electron microscopy experiments will provide a powerful tool to further advance our knowledge and understanding of heme uptake and localization in not only *C. elegans,* but also in parasitic worms.

REFERENCES

1. Tsiftsoglou, A. S., Tsamadou, A. I., and Papadopoulou, L. C. (2006). Heme as key regulator of major mammalian cellular functions: molecular, cellular, and pharmacological aspects. *Pharmacol Ther*, 111: 327-45.
2. Mense, S. M., and Zhang, L. (2006). Heme: a versatile signaling molecule controlling the activities of diverse regulators ranging from transcription factors to MAP kinases. *Cell Res*, 16: 681-92.
3. Faller, M., Matsunaga, M., Yin, S., Loo, J. A., and Guo, F. (2007). Heme is involved in microRNA processing. *Nat Struct Mol Biol*, 14: 23-9.
4. Hamza, I., Chauhan, S., Hassett, R., and O'Brian, M. R. (1998). The bacterial irr protein is required for coordination of heme biosynthesis with iron availability. *J Biol Chem*, 273: 21669-74.
5. Todd, B. L., Stewart, E. V., Burg, J. S., Hughes, A. L., and Espenshade, P. J. (2006). Sterol regulatory element binding proteinis a principal regulator of anaerobic gene expression in fission yeast. *Mol. Cell. Biol.*, 26: 2817-2831.
6. Kaasik, K., and Lee, C. C. (2004). Reciprocal regulation of haem biosynthesis and the circadian clock in mammals. *Nature*, 430: 467-71.
7. Wyllie, J. C., and Kaufman, N. (1982). An electron microscopic study of heme uptake by rat duodenum. *Lab Invest*, 47: 471-6.
8. Parmley, R. T., Barton, J. C., Conrad, M. E., Austin, R. L., and Holland, R. M. (1981). Ultrastructural cytochemistry and radioautography of hemoglobin--iron absorption. *Exp Mol Pathol*, 34: 131-44.

9. Weissman, Z., and Kornitzer, D. (2004). A family of Candida cell surface haem-binding proteins involved in haemin and haemoglobin-iron utilization. *Mol Microbiol*, 53: 1209-20.

10. Kabe, Y., Ohmori, M., Shinouchi, K., Tsuboi, Y., Hirao, S., Azuma, M., Watanabe, H., Okura, I., and Handa, H. (2006). Porphyrin accumulation in mitochondria is mediated by 2-oxoglutarate carrier. *J Biol Chem*, 281: 31729-31735.

11. Quigley, J. G., Yang, Z., Worthington, M. T., Phillips, J. D., Sabo, K. M., Sabath, D. E., Berg, C. L., Sassa, S., Wood, B. L., and Abkowitz, J. L. (2004). Identification of a human heme exporter that is essential for erythropoiesis. *Cell*, 118: 757-66.

12. Krishnamurthy, P. C., Du, G., Fukuda, Y., Sun, D., Sampath, J., Mercer, K. E., Wang, J., Sosa-Pineda, B., Murti, K. G., and Schuetz, J. D. (2006). Identification of a mammalian mitochondrial porphyrin transporter. *Nature*, 443: 586-9.

13. Rao, A. U., Carta, L. K., Lesuisse, E., and Hamza, I. (2005). Lack of heme synthesis in a free-living eukaryote. *Proc Natl Acad Sci U S A*, 102: 4270-5.

14. Granick, S., and Levere, R. D. (1965). The intracellular localization of heme by a fluorescence technique *J. Cell Biol.*, 26: 167-176.

15. Lara, F. A., Lins, U., Bechara, G. H., and Oliveira, P. L. (2005). Tracing heme in a living cell: hemoglobin degradation and heme traffic in digest cells of the cattle tick Boophilus microplus. *J Exp Biol*, 208: 3093-101.

16. Liem, H. H., Tavassoli M., Muller-Eberhard, U. (1975). Cellular and

subcellular localization of heme and hemopexin in the rabbit. *Acta Haematology*, 53: 219-225.

17. Graham, R. C., Jr., Karnovsky, MJ (1966). The early stages of absorption of injected horseradish peroxidase in the proximal tubules of mouse kidney: ultrastructural cytochemistry by a new technique. *J. Histochem. Cytochem.*, 14: 291-302.

18. Ajioka, R. S., Phillips, J. D., and Kushner, J. P. (2006). Biosynthesis of heme in mammals. *Biochim Biophys Acta*, 1763: 723-36.

19. Barros, M. H., Nobrega, F. G., and Tzagoloff, A. (2002). Mitochondrial ferredoxin is required for heme A synthesis in Saccharomyces cerevisiae. *J Biol Chem*, 277: 9997-10002.

20. Morrison, M. S., Cricco, J.A., Hegg, E.L. (2005). The biosynthesis of heme O and heme A is not regulated by copper. *Biochemistry*, 44: 12554-12563.

21. Moraes, C. T., Diaz, F., and Barrientos, A. (2004). Defects in the biosynthesis of mitochondrial heme c and heme a in yeast and mammals. *Biochim Biophys Acta*, 1659: 153-9.

22. Li, J. M., Brathwaite, O., Cosloy, S.D., Russell, C.S (1989). 5-aminolevulinic acid synthesis in escherichia coli. *Journal of Bacteriology*, 171: 2547-2552.

23. Panek, H., and O'Brian, M. R. (2002). A whole genome view of prokaryotic haem biosynthesis. *Microbiology*, 148: 2273-82.

24. Nakajima, O., Takahashi, S., Harigae, H., Furuyama, K., Hayashi, N., Sassa, S., and Yamamoto, M. (1999). Heme deficiency in erythroid lineage causes differentiation arrest and cytoplasmic iron overload. *Embo J*, 18: 6282-9.

25. Dioum, E. M., Rutter, J., Tuckerman, J. R., Gonzalez, G., Gilles-Gonzalez, M.-A., and McKnight, S. L. (2002). NPAS2: A gas-responsive transcription factor. *Science*, 298: 2385-2387.

26. Gilles-Gonzalez, M.-A., and Gonzalez, G. (2005). Heme-based sensors: defining characteristics, recent developments, and regulatory hypotheses. *Journal of Inorganic Biochemistry*, 99: 1-22.

27. Han, L., Lu, J., Pan, L., Wang, X., Shao, Y., Han, S., and Huang, B. (2006). Histone acetyltransferase p300 regulates the transcription of human erythroid-specific 5-aminolevulinate synthase gene. *Biochemical and Biophysical Research Communications*, 348: 799-806.

28. Melefors, O., Goossen, B., Johansson, H.E., Stripecke, R., Gray, N., Hentze, M.W. (1993). Translational control of 5-aminolevulinate synthase mRNA by iron-responsive elements in erythroid cells. *The Journal of Biological Chemistry*, 268: 5974-5978.

29. Cooperman, S. S., Meyron-Holtz, E. G., Olivierre-Wilson, H., Ghosh, M. C., McConnell, J. P., and Rouault, T. A. (2005). Microcytic anemia, erythropoietic protoporphyria, and neurodegeneration in mice with targeted deletion of iron-regulatory protein 2. *Blood*, 106: 1084-1091.

30. Dwyer, B. E., Stone, M. L., Zhu, X., Perry, G., and Smith, M. A. (2006). Heme deficiency in Alzheimer's disease: a possible connection to porphyria. *J Biomed Biotechnol*, 2006: 24038.

31. Oates, P. S., and West, A. R. (2006). Heme in intestinal epithelial cell turnover, differentiation, detoxification, inflammation, carcinogenesis,

absorption and motility. *World J Gastroenterol*, 12: 4281-95.

32. Hughes, A. L., Powell, D. W., Bard, M., Eckstein, J., Barbuch, R., Link, A. J., and Espenshade, P. J. (2007). Dap1/PGRMC1 binds and regulates cytochrome P450 enzymes. *Cell Metabolism*, 5: 143-149.

33. Fayadat, L., Niccoli-Sire, P., Lanet, J., and Franc, J.-L. (1999). Role of heme in intracellular trafficking of thyroperoxidase and Involvement of H2O2 generated at the apical surface of thyroid cells in autocatalytic covalent heme binding. *J. Biol. Chem.*, 274: 10533-10538.

34. Ye, W., and Zhang, L. (2004). Heme controls the expression of cell cycle regulators and cell growth in HeLa cells. *Biochem Biophys Res Commun*, 315: 546-54.

35. Maywood, E. S., Mrosovsky, N., Field, M. D., and Hastings, M. H. (1999). Rapid down-regulation of mammalian Period genes during behavioral resetting of the circadian clock. *PNAS*, 96: 15211-15216.

36. Davies, B. S. J., and Rine, J. (2006). A role for sterol levels in oxygen sensing in saccharomyces cerevisiae. *Genetics*, 174: 191-201.

37. Shan, Y., Lambrecht, R. W., Ghaziani, T., Donohue, S. E., and Bonkovsky, H. L. (2004). Role of Bach-1 in regulation of heme oxygenase-1 in human liver cells: insights from studies with small interfering RNAS. *J Biol Chem*, 279: 51769-74.

38. Genco, C. A., and Dixon, D. W. (2001). Emerging strategies in microbial haem capture. *Mol Microbiol*, 39: 1-11.

39. Latunde-Dada, G. O., Simpson, R. J., and McKie, A. T. (2006). Recent

advances in mammalian haem transport. *Trends Biochem Sci*, 31: 182-8.

40. Wandersman, C., and Delepelaire, P. (2004). BACTERIAL IRON SOURCES: From Siderophores to Hemophores. *Annual Review of Microbiology*, 58: 611-647.

41. Skaar, E. P., Humayun, M., Bae, T., DeBord, K. L., and Schneewind, O. (2004). Iron-source preference of Staphylococcus aureus infections. *Science*, 305: 1626-8.

42. Brickman, T. J., Vanderpool, C. K., and Armstrong, S. K. (2006). Heme transport contributes to in vivo fitness of Bordetella pertussis during primary infection in mice. *Infect Immun*, 74: 1741-4.

43. Wyckoff, E. E., Lopreato, G. F., Tipton, K. A., and Payne, S. M. (2005). Shigella dysenteriae ShuS promotes utilization of heme as an iron source and protects against heme toxicity. *J. Bacteriol.*, 187: 5658-5664.

44. Santos, R., Buisson, N., Knight, S., Dancis, A., Camadro, J. M., and Lesuisse, E. (2003). Haemin uptake and use as an iron source by Candida albicans: role of CaHMX1-encoded haem oxygenase. *Microbiology*, 149: 579-88.

45. Pendrak, M. L., Chao, M. P., Yan, S. S., and Roberts, D. D. (2004). Heme oxygenase in Candida albicans is regulated by hemoglobin and is necessary for metabolism of exogenous heme and hemoglobin to alpha-biliverdin. *J Biol Chem*, 279: 3426-33.

46. Colley, D. G., LoVerde, P. T., and Savioli, L. (2001). Infectious disease. Medical helminthology in the 21st century. *Science*, 293: 1437-1438.

47. Sangster, N. C., and Gill, J. (1999). Pharmacology of anthelmintic resistance.

Parasitol Today, 15: 141-6.

48. Held, M. R., Bungiro, R. D., Harrison, L. M., Hamza, I., and Cappello, M. (2006). Dietary iron content mediates hookworm pathogenesis in vivo. *Infect Immun*, 74: 289-95.

49. Foster, J., Ganatra, M., Kamal, I., Ware, J., Makarova, K., Ivanova, N., Bhattacharyya, A., Kapatral, V., Kumar, S., Posfai, J., Vincze, T., Ingram, J., Moran, L., Lapidus, A., Omelchenko, M., Kyrpides, N., Ghedin, E., Wang, S., Goltsman, E., Joukov, V., Ostrovskaya, O., Tsukerman, K., Mazur, M., Comb, D., Koonin, E., and Slatko, B. (2005). The Wolbachia genome of Brugia malayi: endosymbiont evolution within a human pathogenic nematode. *PLoS Biol*, 3: e121.

50. Krishnamurthy, P., and Schuetz, J. D. (2005). The ABC transporter Abcg2/Bcrp: role in hypoxia mediated survival. *Biometals*, 18: 349-58.

51. Jonker, J. W., Buitelaar, M., Wagenaar, E., van der Valk, M. A., Scheffer, G. L., Scheper, R. J., Plosch, T., Kuipers, F., Elferink, R. P. J. O., Rosing, H., Beijnen, J. H., and Schinkel, A. H. (2002). The breast cancer resistance protein protects against a major chlorophyll-derived dietary phototoxin and protoporphyria. *PNAS*, 99: 15649-15654.

52. Hamza, I. (2006). Intracellular trafficking of porphyrins. *ACS Chem Biol*, 1: 627-9.

53. Qiu, A., Jansen, M., Sakaris, A., Min, S. H., Chattopadhyay, S., Tsai, E., Sandoval, C., Zhao, R., Akabas, M. H., and Goldman, I. D. (2006). Identification of an intestinal folate transporter and the molecular basis for

hereditary folate malabsorption. *Cell*, 127: 917-28.

54. Lara, F. A., Lins, U., Paiva-Silva, G., Almeida, I. C., Braga, C. M., Miguens, F. C., Oliveira, P. L., and Dansa-Petretski, M. (2003). A new intracellular pathway of haem detoxification in the midgut of the cattle tick Boophilus microplus: aggregation inside a specialized organelle, the hemosome. *J Exp Biol*, 206: 1707-1715.

55. Xie, G., Jia, Y., and Aamodt, E. (1995). A C. elegans mutant screen based on antibody or histochemical staining. *Genet Anal*, 12: 95-100.

56. Sciacco, M., and Bonilla, E. (1996). Cytochemistry and immunocytochemistry of mitochondria in tissue sections. *Methods Enzymol*, 264: 509-21.

57. Paupard, M. C., Miller, A., Grant, B., Hirsh, D., and Hall, D. H. (2001). Immuno-EM localization of GFP-tagged yolk proteins in C. elegans using microwave fixation. *J Histochem Cytochem*, 49: 949-56.

58. Brenner, S. (1974). The genetics of Caenorhabditis elegans. *Genetics*, 77: 71-94.

59. Grad, L. I., and Lemire, B. D. (2004). Mitochondrial complex I mutations in Caenorhabditis elegans produce cytochrome c oxidase deficiency, oxidative stress and vitamin-responsive lactic acidosis. *Hum. Mol. Genet.*, 13: 303-314.

60. Simionescu, N., Simionescu, M., and Palade, G. E. (1973). Permeability of muscle capillaries to exogenous myoglobin *J. Cell Biol.*, 57: 424-452.

61. Kachur, T., Ao, W., Berger, J., and Pilgrim, D. (2004). Maternal UNC-45 is involved in cytokinesis and colocalizes with non-muscle myosin in the early Caenorhabditis elegans embryo. *J Cell Sci*, 117: 5313-5321.

62. Kamping, A., Katju, V., Beukeboom, L. W., and Werren, J. H. (2006). Inheritance of gynandromorphism in the parasitic wasp Nasonia vitripennis. *Genetics*: genetics.106.067082.

63. Garamszegi, L. Z., Biard, C., Eens, M., Moller, A. P., Saino, N., and Surai, P. Maternal effects and the evolution of brain size in birds: Overlooked developmental constraints. *Neuroscience & Biobehavioral Reviews*, In Press, Corrected Proof.

64. Giordano, M., and Momigliano-Richiardi, P. (2004). Maternal effect in multiple sclerosis. *The Lancet*, 363: 1748-1749.

65. Fukushige, T., Goszczynski, B., Yan, J., and McGhee, J. D. (2005). Transcriptional control and patterning of the pho-1 gene, an essential acid phosphatase expressed in the C. elegans intestine. *Developmental Biology*, 279: 446-461.

66. Burgess, J., Hihi, A. K., Benard, C. Y., Branicky, R., and Hekimi, S. (2003). Molecular mechanism of maternal rescue in the clk-1 mutants of Caenorhabditis elegans. *J. Biol. Chem.*, 278: 49555-49562.